JPET Fast Forward. Published on September 21, 2020 as DOI: 10.1124/jpet.120.000047
This article has not been copyedited and formatted. The final version may differ from this version.

JPET-AR-2020-000047

Targeted Injection of a Truncated Form of Tissue Inhibitor of Metalloproteinase 3 Alters Post-MI Remodeling

David C. Lobb, PhD[+], Heather Doviak, BS[+], Gregory L. Brower, PhD[+], Eva Romito, PhD[+], Jason W. O'Neill, PhD[§], Stephen Smith, PhD[§], James A. Shuman, MD[+], Parker D. Freels, MD[+], Kia N. Zellars, BS[+], Lisa A. Freeburg, BS[+], Aarif Y. Khakoo, MD[§], TaeWeon Lee, PhD[§], Francis G. Spinale, MD, PhD[+]

[+]Cardiovascular Translational Research Center, University of South Carolina School of Medicine and the WJB Dorn Veteran Affairs Medical Center, Columbia, SC; [§] Amgen, Metabolic Disorders, South San Francisco, CA

Conflict Statement

JWO, SS, AK, and TL are employees of Amgen Inc. that manufacture drugs for a wide range of diseases, including cardiovascular disease. The other authors declare that they have no competing interests. The recombinant TIMP-3 formulations were furnished as an MTA from Amgen to FGS.

JPET Fast Forward. Published on September 21, 2020 as DOI: 10.1124/jpet.120.000047
This article has not been copyedited and formatted. The final version may differ from this version.

Running Title: TIMP-3 domains and post-MI remodeling

Address for Correspondence:
Francis G. Spinale, MD, PhD
CBA, University of South Carolina School of Medicine
6439 Garners Ferry Road
Building 3, Room 234
Columbia, SC 29208
Phone: 803-216-3880
Email:cvctrc@uscmed.sc.edu

Manuscript Statistics
Pages: 27
Figures: 8
Total Word Count: 5322
Abstract: 229
Introduction: 489
Discussion: 1396 (less citations)
Supplemental Material: 4

Table of Abbreviations

ANOVA	Analysis of variance
COL1A1	Collagen type I
COL3A1	Collagen type III
Ct	Cycle times
ECM	Extracellular matrix
F-TIMP-3	Full-length recombinant TIMP-3
IL	Interleukins
LA	Left atrial
LV	Left ventricular
MCP1	Monocyte chemoattractant protein-1
MI	Myocardial infarction
MIP1A	Macrophage inflammatory protein-1 alpha
MMP	Matrix metalloproteinase
mRNA	Messenger RNA
N-TIMP-3	N-terminal region TIMP-3
PSR	Picrosirius red
SEM	Standard effort of the mean
SMA	Smooth muscle actin
TFF	Tangential flow filtration
TIMP	Tissue inhibitor of metalloproteinase
TNFα	Tumor necrosis factor alpha

Recommended section assignment: cardiovascular

JPET Fast Forward. Published on September 21, 2020 as DOI: 10.1124/jpet.120.000047
This article has not been copyedited and formatted. The final version may differ from this version.

Abstract

Infarct expansion can occur after myocardial infarction (MI), which leads to adverse left ventricular (LV) remodeling and failure. An imbalance between matrix metalloproteinase (MMP) induction and tissue inhibitors of MMPs (TIMPs) can accelerate this process. Past studies have shown different biological effects of TIMP-3, which may depend upon specific domains within the TIMP-3 molecule This study tested the hypothesis that differential effects of direct myocardial injections of either a full length recombinant TIMP-3 (F-TIMP-3) or a truncated form encompassing the N-terminal region (N-TIMP-3) could be identified post-MI. MI was induced in pigs and randomized for MI injections (30 mg) and received targeted injections within the MI region of F-TIMP-3 (n=8), N-TIMP-3 (n=9), or saline injection (MI-only, n=11). At 14 days post-MI, LV ejection fraction fell post-MI but remained higher in both TIMP-3 groups. Tumor necrosis factor and interleukin-*10* mRNA increased by over 10-fold in the MI only and N-TIMP-3 groups but were reduced with F-TIMP-3 at this post-MI time point. Direct MI injection of either a full length or truncated form of TIMP-3 is sufficient to favorably alter the course of post-MI remodeling. The functional and differential relevance of TIMP-3 domains has been established *in-vivo* since the TIMP-3 constructs demonstrated different MMP/cytokine expression profiles. These translational studies identify a unique and more specific therapeutic strategy to alter the course of LV remodeling and dysfunction following MI.

JPET Fast Forward. Published on September 21, 2020 as DOI: 10.1124/jpet.120.000047
This article has not been copyedited and formatted. The final version may differ from this version.

Significance Statement

Using different TIMP-3 formulations, when injected into the MI region, slowed the progression of indices of LV failure, suggesting that the N terminus of TIMP-3 is sufficient to attenuate early adverse functional events post-MI. The F-TIMP-3 injections but not N-TIMP-3 injections reduced relative indices of inflammation at the mRNA level, suggesting that the C-terminus region affects other biological pathways. These unique proof of concept studies demonstrate the feasibility of using recombinant small molecules to selectively interrupt adverse LV remodeling post-MI.

JPET Fast Forward. Published on September 21, 2020 as DOI: 10.1124/jpet.120.000047
This article has not been copyedited and formatted. The final version may differ from this version.

Introduction

A structural milestone in the progression of heart failure following a myocardial infarction (MI) is left ventricular (LV) remodeling, which can be defined as changes in LV geometry and structure. (Konstam et al, 2011; Spinale FG, 2007; Sutton and Sharpe, 2000; Weir et al, 2006) Specifically, this adverse remodeling process is characterized by continuous turnover of the extracellular matrix (ECM) within the MI region, causing mural wall thinning, LV chamber dilation, and eventually pump dysfunction.(Lindsey and Zamilpa, 2012; Mukherjee et al, 2003; Spinale, 2007) One biological system that is active in the post-MI context is a family of ECM proteases, the matrix metalloproteinases (MMPs),(Lindsey and Zamilpa, 2012; Mukherjee et al, 2003; Spinale, 2007) whereby induction and release of MMPs has been demonstrated in patients post-MI and associated with adverse LV remodeling.(Webb et al, 2006) Basic studies utilizing transgenic constructs or pharmacological strategies provided mechanistic evidence that modulating MMP activity would favorably alter the course of post-MI remodeling.(Heymans et al, 1999; Kandalam et al, 2010; Lindsey et al, 2002; Lindsey and Zamilpa, 2012; Mukherjee et al, 2003; Spinale, 2007) However, clinical translation of these studies have encountered problematic issues, which include the ability of systemic delivery of pharmacological MMP inhibitors reaching therapeutic levels and concerns regarding off-target effects.(Dorman et al, 2010; Hudson et al, 2006; Peterson, 2004) An alternative therapeutic approach would be to target MMP activity within the MI region specifically and thus avoid potential systemic effects. Accordingly, this project utilized a relevant large animal post-MI model (Dixon and Spinale, 2009) and a localized targeted approach to interfere with MMP proteolytic activity. Endogenous MMP inhibition is achieved through the synthesis and release of the tissue inhibitors of MMPs (TIMPs).(Bourboulia and Stetler-Stevenson, 2010; Brew and Nagase, 2010; Douglas et al, 1997) There are four known TIMPs, and past studies have identified that a relative MMP/TIMP imbalance occurs within the MI region, thus favoring ECM proteolysis and instability and post-MI remodeling.(Lindsey and Zamilpa, 2012; Mukherjee et al, 2003; Peterson et al, 2000; Spinale, 2007; Wilson et al, 2003) However, the effects of individual TIMPs are not uniform in terms of MMP inhibitory profiles, processing of biological signaling cascades, and effects upon growth/proliferation/viability.(Abbate et al, 2002; Hammoud et al, 2009; Lovelock et al, 2005; Lu et al, 2011; Melendez-Zajgla et al, 2008; Troeberg et al, 2009) For example, unique features of TIMP-3 include a high affinity to bind to the ECM,(Leco et al, 1994; Yu et al, 2000)

an influence on cytokine processing,(Bourboulia and Stetler-Stevenson, 2010; Brew and Nagase, 2010; Troeberg et al, 2009) and altering fibroblast phenotype *in-vitro*.(Lovelock et al, 2005; Shinde and Frangogiannis, 2014; Yang and Hawkes, 1992) Moreover, transgenic deletion of TIMP-3 causes adverse remodeling, acceleration to heart failure, and reduced survival.(Hammoud et al, 2011; Kandalam et al, 2010) These previous studies provide a strong rationale for pursuing the concept that augmentation of TIMP-3 would be a potential therapeutic strategy post-MI. Specifically, this project was developed around the central hypothesis that a localized, targeted augmentation of TIMP-3 within the MI region would favorably alter adverse LV remodeling. Thus, the first objective of this study was to directly inject a full length recombinant TIMP-3 into the MI region and quantify the effects upon the natural history of post-MI remodeling.

The structural domains of TIMPs can be divided into the N-terminal and C-terminal subdomains, whereby the global MMP inhibitory component appears to reside in the N-terminal domain.(Brew and Nagase, 2010; Douglas et al, 1997) With respect to TIMP-3, past *in-vitro* studies have demonstrated that mutations within the N-terminal domain while altering MMP inhibitory effects did not alter proteolytic mediated cytokine processing.(Wei et al, 2005) These studies would lead to postulate that the N-terminal domain of TIMP-3 may be sufficient to blunt MMP activity and hence modify post-MI remodeling. Accordingly, the second objective of this study was to perform targeted injections of a truncated form of TIMP-3 containing the N-terminal domain and perform comparative studies of post-MI remodeling.

JPET Fast Forward. Published on September 21, 2020 as DOI: 10.1124/jpet.120.000047
This article has not been copyedited and formatted. The final version may differ from this version.

Methods

In this study, both a full-length TIMP-3 recombinant protein, referred to as F-TIMP-3, and a truncated form of TIMP-3 containing the N-domain of TIMP-3, referred to as N-TIMP-3, were utilized. The TIMP-3 structure and sequences for these constructs are shown in Figure 1A and the methodology for the construction of these TIMP-3 variants is provided in Supplemental Methods. Initial *in-vitro* and *in-vivo* studies were performed to validate the TIMP-3 formulations in terms of MMP inhibition and myocardial localization as provided in detail in the Supplemental Methods. Briefly, using an MMP fluorescent peptide assay,(Spinale et al, 2008) inhibition in MMP activity occurred with increasing concentrations of either F-TIMP-3 or N-TIMP-3 (Figure 1B) with an approximate 50% inhibitory concentration (IC_{50}) of 2-6 ug/mL (0.4-5 nM), indicative that both proteins inhibited MMP activity in the manner consistent with native TIMP-3.(Douglas et al, 1997) Studies were then carried out to develop a dose and localization of the F-TIMP-3 or N-TIMP-3 injections. In the subsequent efficacy studies, equivalent concentrations of the TIMP-3 formulations were injected into the MI region in order to examine the effects on LV geometry and function. For the animal model, adult pigs were utilized as MI induction in this species results in uniformity of MI size and temporal changes in LV geometry.(Dixon and Spinale, 2009; Eckhouse et al, 2014; Mukherjee et al, 2003; Mukherjee et al, 2008) All animals were treated and cared for in accordance with the National Institutes of Health *Guide for the Care and Use of Laboratory Animals* (*Eighth Edition*. Washington, DC: 2011), and all protocols were approved by the University of South Carolina's Institutional Animal Care and Use Committee. Serial studies were carried out until 14 days post-MI as this time period encompasses a rapid change in LV geometry and function in both animals and patients.(Mukherjee et al, 2003; Webb et al, 2006) Following the final set of LV function measurements, sections of the MI region were subjected to mRNA analysis for MMP/TIMP and cytokine levels as well as histochemistry.

Development of TIMP-3 Myocardial Injection Strategy and Validation

Targeted myocardial injections of the TIMP-3 formulations were performed within the LV free wall of mature pigs (25kg, Yorkshire, Hambone Farms, Orangeburg, SC). The pigs (n=10) were anesthetized with isoflurane (2%), and through a left thoracotomy, the LV free wall was exposed. A 6-point injection grid (2X2 cm, uniform point distances of 0.5 cm) was temporarily

JPET Fast Forward. Published on September 21, 2020 as DOI: 10.1124/jpet.120.000047
This article has not been copyedited and formatted. The final version may differ from this version.

sutured to the epicardial surface below the origin of the first two obtuse marginal arteries of the circumflex artery (schematic shown in Figure 1C). This targeted injection region is contained within the myocardial region for coronary ligation and subsequent MI induction. The F-TIMP-3 or N-TIMP-3 formulations were diluted in sterile saline in order to provide final concentrations of 2, 5, or 10 mg/100 uL (injection site volume 100 uL, 6 injection sites; total injection volume 600 uL; BD Ultra-Fine^{TM} 31G). The specific approaches and results from these studies are provided in Supplemental Methods. Using these results, and to ensure dosing equivalency with respect to mass/volume, a 5 mg/injection dose was selected for subsequent *in-vivo* studies. Using the 6-point injection pattern yielded a total myocardial delivery of 30 mg of either F- or N-TIMP-3. While absolute myocardial concentration computations require several assumptions, the total injected myocardial region was 4 mL (2X2X1 cm, specific gravity of 1 cm^3/mL), resulting in an initial delivery of 750 ug/mL, thus reflective of a 100X concentration from the computed EC_{50} for the TIMP formulations.

The next set of studies more carefully examined the spatial distribution and temporal retention of the TIMP-3 formulations in the targeted myocardial injection region. Specifically, F-TIMP-3 or N-TIMP-3 were fluorescently labelled as detailed in the Supplemental Methods. Pigs (25 kg, n=12) underwent targeted myocardial injections of fluorescently labelled F-TIMP-3 or N-TIMP-3 (6 injection pattern) as described in the previous section, whereby the LV was harvested immediately post-injection or at 3 and 5 days post-injection, and circumferential LV sections were subjected to epi-illumination imaging as detailed in the Supplemental Methods. A representative set of LV images from each region with injection of each TIMP-3 formulation immediately following injection and at 3 and 5 days post-injection is shown in Figure 1D. Using an exponential fit model, the computed F-TIMP-3 retention half-life was approximately 8 days, and for N-TIMP-3, it was approximately 6 days.

MI Induction and TIMP-3 Injections - Randomization and Uniformity in MI Size

For this protocol, pigs (n=26, 20 kg, male) were randomized to one of three different groups: MI and saline injections (MI/saline; 100 uL injection/6 injection sites, n=9), MI and F-TIMP-3 injections (MI/F-TIMP-3; 30 mg total injection, n=8), MI and N-TIMP-3 (MI/N-TIMP-3; 30 mg total injection, n=9). The pigs were randomized prior to surgery using a random number table, and the treatment code was not broken until the completion of the entire protocol and

JPET Fast Forward. Published on September 21, 2020 as DOI: 10.1124/jpet.120.000047
This article has not been copyedited and formatted. The final version may differ from this version.

analysis. The pigs were anesthetized as described in the previous section, and following a thoracotomy, a vascular access catheter (6 Fr, Access Technologies) was placed in the thoracic aorta and attached to a subcutaneous port for blood sample collection and measurement of troponin I (ELISA, Kamiya Biomedical Company, Seattle, WA, Cat #KT-641). Plasma troponin I measurements were obtained prior to MI induction (Baseline), at 24 hours, 72 hours post-MI, as well as at 14 days post-MI. MI induction was achieved by ligating the obtuse marginal branch 1 (OM1) and 2 (OM2) at the origin just below the circumflex artery as described previously.(Mukherjee et al, 2008) A cohort (n=5) of age/weight matched pigs were treated in identical fashion (sham procedures) and served as referent controls for myocardial biochemistry and histology.

Serial Measurements of LV Geometry and Function, Referent Controls, and Sampling

An outline of the experimental design is shown in Figure 2A with the sampling points identified. The day before randomization and MI induction, the animals were sedated (diazepam, 200mg-PO, Barr Laboratories, Pomona, NY) and echocardiography performed (GE VIVID 7 Dimension Ultrasound System: M4S 1.5-4.3 MHz active matrix array sector transducer probe) in order to measure LV volumes, left atrial (LA) area, posterior LV free wall thickness, and ejection fraction as described previously.(Eckhouse et al, 2014; Mukherjee et al, 2003; Mukherjee et al, 2008) In addition, mitral valve inflow velocities and tissue Doppler were used to compute an estimate of pulmonary capillary wedge pressure.(Zile et al, 2011) The pigs were returned to the laboratory under identical sedation/study conditions at 1, 3, 7, and 14 days post-MI. At the completion of the study interval, the pigs were again anesthetized and the LV region containing the MI region harvested.

Myocardial MMP/TIMP/cytokine mRNA, Histochemistry, and MMP Activity

RNA was extracted from the LV samples (Experion Automated Electrophoresis System; Bio-Rad Laboratories, Hercules, CA), reverse transcribed (iScript cDNA Synthesis Kit; Bio-Rad, Hercules, CA), and cDNA amplified with gene/pig specific primer/probe sets (RT^2 Profiler PCR Custom Array, Qiagen), which is presented in Supplemental Table 1. The array was designed to contain primers for representative MMP types, all four TIMPs, the fibrillar collagens (collagen I and III), as well as inflammatory cytokines identified to be relevant to

JPET Fast Forward. Published on September 21, 2020 as DOI: 10.1124/jpet.120.000047
This article has not been copyedited and formatted. The final version may differ from this version.

post-MI remodeling.(Dewald et al, 2005; Frangogiannis, 2012) In addition, indices of the Bcl-2 family, which regulate mitochondrial apoptotic factors, Bcl-2 associated protein (BAX), and B-cell lymphoma 2 (BCL2) were also included in this analysis.(Abbate et al, 2002) The reaction was performed (RT^2 SYBR Green@qPCR Mastermix, Qiagen) and quantified by real time (CFX96 real-time PCR detection system, Bio-Rad, Hercules, CA). In addition to the targeted PCR measurements, a large porcine cytokine/receptor PCR array was utilized (330231 PASS-011ZD, Qiagen), which contained 84 inflammatory cytokines and cytokine receptors (Supplemental Table 2). The real time PCR fluorescence signal was converted to cycle times (Ct) normalized to GAPDH (ΔCt). All PCR assays were performed in duplicate.

LV samples were formalin fixed, embedded, sectioned (7 um), and stained with H&E and picrosirius red (PSR) for fibrillar collagen, whereby the percent area of collagen was computed using computer assisted morphometry (Nikon E600 with Q imaging software and Image-Pro Plus Version 4.5). For both the MI and remote LV sections, an average of 15 random fields were digitized from 3 independent sections and computed as a composite value for each pig. Additional LV sections were stained with hematoxylin and eosin, and histopathological examination of the targeted MI region was performed. Additional LV sections were used for immunostaining to localize cells that stained positive for α-smooth muscle actin (SMA; 1:100; α-smooth muscle actin: Sigma A5228) as well as for macrophages using a previously validated antisera in porcine formalin fixed tissue (IBA-1; 1:2000; Wako Chemicals 019-19741).(Bolz et al, 2016) Using quantitative morphometry, the percent area staining for SMA and IBA-1 were computed for both the MI and remote regions.

LV samples from the MI region were homogenized and subjected to MMP activity assays using the global MMP substrate described in the previous section. Briefly, LV samples were homogenized using ice cold buffer (Cacodylic Acid (10 mM/L), NaCl (0.15 M/L), ZnCl (20 mM/L), NaN_3 (1.5 mM/L), and 0.01% Triton X-100 (pH 5.0)), centrifuged, and LV extracts (10 µg; Pierce BCA Protein Assay Kit; Thermo Scientific, Cat #23225) incubated at 37°C with the global MMP substrate (37°C for 6hrs), and fluorescence recorded. Using the same conditions, LV extracts (10 µg) were also incubated with a fluorogenic MT1-MMP specific substrate (0.06 µM, Millipore, Cat #444258) and fluorescence measured at 6 hours (328/400 nm; FLUOstar, BMG Laboratories).

JPET Fast Forward. Published on September 21, 2020 as DOI: 10.1124/jpet.120.000047
This article has not been copyedited and formatted. The final version may differ from this version.

Computation and Data Analysis

Statistical analyses were performed (STATA Corp, College Station, TX), whereby LV geometry and function initially examined by a two-way analysis of variance (ANOVA) in which time and treatment were considered main effects. Post-hoc separation following ANOVA was performed using pairwise comparisons with a least-significant analysis (LSD module, STATA). If the assumption regarding equal variances between groups or normality in the data distribution were not met, then a non-parametric pairwise comparison between groups at matched time points was performed using Wilcoxon (nonparametric module, STATA). For example, this was encountered for the cytokine mRNA measurements. Results are presented as a mean ± standard error of the mean (SEM) and values of $p<0.05$ were considered to be statistically significant.

JPET Fast Forward. Published on September 21, 2020 as DOI: 10.1124/jpet.120.000047
This article has not been copyedited and formatted. The final version may differ from this version.

Results

TIMP-3 Injections Attenuate Adverse LV Remodeling Post-MI

Plasma troponin I values were equivalent across the randomized treatment groups (Figure 3). Specifically, a significant and equivalent surge in plasma troponin I occurred at 24 hours post-MI and returned to near Baseline values in all groups at later post-MI time points. Thus, a uniform and consistent magnitude of myocardial injury was induced and thereby removed this potential confounding factor from the experimental design. Key indices of LV function and geometry are shown in Figure 3. Representative LV echocardiograms are shown in Figure 2B and a summary of key indices of LV function and geometry are shown in Figure 3. LV end-diastolic volume, a reflection of post-MI remodeling, increased in a time dependent manner post-MI in all groups but was reduced in both the F-TIMP-3 and N-TIMP-3 groups at later post-MI time points. LV posterior wall thickness, another index of MI remodeling, decreased in a time dependent manner post-MI but was attenuated in both TIMP-3 injection groups. LV ejection fraction, a measure of global pump performance, fell significantly post-MI, and this impairment in LV pump function was improved in both TIMP-3 groups. Left atrial area, which reflects changes in LV filling pressure and remodeling, increased post-MI but was reduced at later post-MI time points in the TIMP-3 injection groups. Similarly, pulmonary capillary wedge pressure, which is reflective of left atrial pressures and hence changes in LV filling and remodeling, increased post-MI and was attenuated at late post-MI time points with the TIMP-3 injections. For all of these measures of LV function and geometry, the ANOVA revealed a significant time-treatment interaction ($p<0.05$), which indicates that TIMP-3 treatment altered the course of post-MI remodeling. While each of the TIMP-3 formulation injections was different from MI/saline values at key post-MI time points, adjusted pair-wise comparisons revealed no differences in these effects between the F-TIMP-3 and N-TIMP-3 formulations.

Differential Effects on MMP/TIMP mRNA Expression with TIMP-3 Injections

Relative mRNA levels for MMP-2, MMP-9, and MMP-14 were robustly increased in the MI/saline group compared to referent control values but were significantly suppressed in the F-TIMP-3 group (Figure 4). In contrast, mRNA levels for these MMP types were similar to MI/saline values in the N-TIMP-3 group. Similarly, mRNA levels for MMP-13 were increased

JPET Fast Forward. Published on September 21, 2020 as DOI: 10.1124/jpet.120.000047
This article has not been copyedited and formatted. The final version may differ from this version.

from referent control values in the MI/Saline and MI/N-TIMP-3 groups (0.9±0.1, 3.7±1.5, 3.3±0.72 $^{-\Delta Ct}$ x10^3, p<0.05 respectively) and fell to control values in the MI/F-TIMP-3 group (0.9±0.1$^{-\Delta Ct}$ x10^3, p<0.05). Relative expression levels for endogenous TIMP-1,-2,-3,-4 were higher than referent control in the MI/saline group and were uniformly reduced in the F-TIMP-3 group (Figure 4). However, in the MI/N-TIMP-3 group, TIMP levels returned to MI/saline values with the notable exception for endogenous TIMP-3, which increased further post-MI.

Differential Effects of mRNA Levels for Collagen/Cytokine/Chemokines and Indices of Apoptosis

A robust increase in fibrillar collagen expression occurred in the MI/saline and MI/N-TIMP-3 groups, which was reduced in the MI/F-TIMP-3 group (Figure 5). Tumor necrosis factor alpha (TNFα) and CD44 mRNA levels increased in all post-MI groups, but relative TNFα expression was lower in the F-TIMP-3 group. Increased chemokine expression, specifically monocyte chemoattractant protein-1 (MCP1 aka chemokine ligand 2) and macrophage inflammatory protein-1 alpha (MIP1A aka chemokine ligand 3-Like 1), increased in all MI groups but were lower in the MI/F-TIMP-3 group (Figure 5). Relative mRNA levels for pro-apoptotic BAX and for the anti-apoptotic BCL2 were both elevated within the MI region but were significantly reduced in the F-TIMP-3 group (Figure 6).

Using the full cytokine array, a very similar pattern emerged. Specifically, when the cytokine and cytokine receptor values were pooled and subjected to ANOVA, a significant treatment effect was observed (F value = 9.6, p<0.001; Figure 7A). Moreover, when subjected to pairwise analysis, overall cytokine expression increased by over 2-fold in the MI/saline group, increased further in the MI/N-TIMP-3 group, and fell to within normal values in the MI/F-TIMP-3 group. Representative selected chemokines, such as (C-C motif) receptor-2 (CCR-2), and interleukins (IL), such IL-8 and IL-10, from this overall array are shown in Figure 4, whereby a very similar pattern of expression was observed. Thus, F-TIMP-3 injections, but not N-TIMP-3 injections, reduced the expression of fibrillar collagen and indices of inflammation post-MI.

LV total MMP activity, reflecting a summation of proteolytic activity of all MMP types, was significantly increased within the MI region of all groups with no difference between groups (Figure 7B). Similarly, MT1-MMP specific activity was increased in all MI groups with a

tendency for higher values in both TIMP-3 treatment groups but did not reach statistical significance (Figure 7C).

Collagen Content and Inflammation following MI; Effects of TIMP-3 Injections

MI sections stained with H&E revealed inflammatory cells and clear regions of scar formation (Figure 8). Qualitative assessment of these stained sections revealed a lower overall inflammatory cell infiltrate in the MI/F-TIMP-3 sections. Clear bands of fibrillar collagen were evident within the MI region with PSR staining (Figure 8). Quantification of MI and remote sections demonstrated equivalent total fibrillar collagen content within the MI region as well as the remote, non-ischemic region for all treatment groups. Thus, while F-TIMP-3 reduced mRNA levels for fibrillar collagen, total collagen content within the MI region remained unaffected, suggesting that changes in post-transcriptional events (i.e. reduced collagen turnover) had occurred. In order to more carefully examine a potential index of myocardial fibroblast phenotype, SMA histochemistry was performed and identified a robust increase within the MI region for all treatment groups. However, the SMA relative content was reduced in the MI/F-TIMP-3 group. Immunostaining for macrophages (IBA-1) revealed a nominal signal in referent control LV sections, which increased significantly in the MI regions of all treatment groups. The density of staining, likely reflective of macrophage density, was reduced in the MI/F-TIMP-3 group but did not reach statistical significance ($p=0.25$). Representative histochemical results for referent normal and post-MI sections from the remote region are provided in Supplemental Figure 1.

JPET Fast Forward. Published on September 21, 2020 as DOI: 10.1124/jpet.120.000047
This article has not been copyedited and formatted. The final version may differ from this version.

Discussion

The post-MI period is invariably accompanied by intense inflammation and extracellular matrix (ECM) remodeling, which is facilitated in part by MMPs.(Heymans et al, 1999; Kandalam et al, 2010; Lindsey et al, 2002; Mukherjee et al, 2003) This in turn causes ECM instability and infarct expansion, which is most commonly identified as an increase in LV end-diastolic volume. While animal models that modify MMP and/or tissue inhibitors of MMPs (TIMPs) have provided a cause-effect relationship to LV remodeling, (Heymans et al, 1999; Kandalam et al, 2010; Lindsey et al, 2002; Lindsey and Zamilpa, 2012; Mukherjee et al, 2003; Spinale, 2007) the translation of these basic findings to potential therapeutic strategies have not been forthcoming. The present study addressed this issue and obtained several unique findings. First, injection of a recombinant TIMP-3 into the MI region imparted a beneficial effect in terms of critical determinants of post-MI LV remodeling. Second, post-MI LV remodeling was attenuated with either F-TIMP-3 or N-TIMP-3, suggesting that the N-terminus region of TIMP-3 is sufficient to attenuate early adverse post-MI remodeling. Third, F-TIMP-3 injections but not N-TIMP-3 injections reduced relative MMP expression and indices of inflammation at the mRNA level, suggesting that the C-terminus region uniquely affects other biological pathways.

The progression of post-MI remodeling include LV chamber dilation, thinning of the LV wall encompassing the MI region, and a reduction in LV systolic function. (Konstam et al, 2011; Spinale, 2007; Sutton and Sharpe, 2000; Weir et al, 2006) The local injection of either a full length or truncated form of TIMP-3 attenuated all of these indices of post-MI remodeling. While both TIMP-3 formulations reduced LV dilation, the post-MI trajectory for this index of LV remodeling appeared to be different between the TIMP-3 formulations. In addition, indices of heart failure progression, (Colucci and Braunwald, 2005; Zile et al, 2011) such as LA size and estimates of pulmonary capillary wedge pressure, were attenuated with F-TIMP-3 or N-TIMP-3 targeted injections. Of note, pulmonary capillary wedge pressure was higher at early post-MI time points with N-TIMP-3 injections, which may have been due to increased myocardial stiffness. However, this remains speculative.

While both TIMP-3 formulations favorably attenuated post-MI remodeling at the chamber/myocardial level, the mechanism(s) for this effect may have been distinctly different. With respect to MMP/TIMP profiles, F-TIMP-3 reduced MMP and TIMP levels within the MI region, whereas N-TIMP-3 appeared to have either no effect on these expression profiles or

JPET Fast Forward. Published on September 21, 2020 as DOI: 10.1124/jpet.120.000047
This article has not been copyedited and formatted. The final version may differ from this version.

arguably caused an amplification of endogenous TIMP-3 levels. However, these changes did not appear to be associated with differences in either global MMP activity or MT1-MMP (MMP-14) specific activity. There are several likely reasons for these observations. Firstly, the retention times for recombinant F-TIMP-3 and N-TIMP-3 were approximately 7 days and the post-MI samples were collected at 14 days. Thus, there was unlikely to be any retained recombinant TIMP formulation in the MI samples subjected to these MMP activity assays. Secondly, with F-TIMP-3, a relatively concordant reduction in both MMPs and endogenous TIMPs occurred at 14 days post-MI and may have resulted in no net effect on overall proteolytic activity when compared to MI-saline values. It should also be noted that MMP activity in and of itself does not reflect ECM stability or turnover.

In the present study, total fibrillar collagen content as assessed by a quantitative histochemical approach was increased within the MI and remote regions at 14 days post-MI and was increased to a similar extent with the different TIMP-3 formulations. However, it should be recognized that this measurement was taken at one point in time and whether and to what degree fibrillar collagen content was affected, particularly within the MI region, at earlier time points with either recombinant TIMP-3 formulation remains unknown. The present study did provide evidence that at the transcriptional level, the recombinant TIMP-3 formulations caused differential effects of fibrillar collagen expression within the MI region. Specifically, F-TIMP-3 reduced collagen type I and III mRNA levels at 14 days post-MI whereas N-TIMP-3 injections did not demonstrate this effect. This underscores the complexity of factors that contribute to fibrillar collagen accumulation within the MI region, and the findings from the present study suggest that certain domains of the TIMP-3 molecule may cause differential effects on the determinants of ECM synthesis and degradation.

A potentially important event is changes in fibroblast phenotype post-MI.(Fu et al, 2018; Khalil et al, 2017; Ma et al, 2013; Ma et al, 2017; Shinde and Frangogiannis, 2014; Wang et al, 2020; Zamilpa et al, 2011) TIMP-3 can influence neonatal mouse proliferation, and TIMP-3 deficiency exacerbated post-MI cardiac rupture and mortality.(Hammoud et al, 2011; Kandalam et al, 2010) It has been established that canonical inflammatory molecules such as TNF can drive fibroblast transdifferentiation.(Awad et al, 2010; Kassiri et al, 2009; Ma et al, 2017) While specific markers of myofibroblasts remain to be fully developed and validated, the identification of SMA expression in these transdifferentiated cells has been utilized.(Awad et al,

2010; Ma et al, 2017) The findings of the present study would suggest that the N-terminal region of N-TIMP-3 was insufficient to attenuate this marker of fibroblast activation post-MI. However, the present study utilized *in-situ* markers for fibroblast activation and future studies utilizing primary myofibroblast cultures, as described in previous studies, (Hammoud et al, 2011; Wang et al, 2020) would add scientific insight to this issue.

It has been shown previously that prolonged inflammation, in particular abnormalities in macrophage activation and polarization, can contribute to adverse post-MI remodeling.(Ma et al, 2013; Zamilpa et al, 2011) The predominant observation from the present study was that F-TIMP-3 injections, but not N-TIMP-3 injections, significantly reduced indices of inflammation. A determinant of macrophage density (CD44) (Frangogiannis, 2012) was selectively reduced by F-TIMP-3 injections. Moreover, markers of macrophage maturation and infiltration, (Dewald et al, 2005) MCP-1 and MIP-1A, increased within the MI region and were markedly lower with F-TIMP-3 injections. It has been reported previously *in-vitro* that distinct functional domains exist within the TIMP-3 molecule that affect ECM proteolytic pathways and that of cytokine processing/induction.(Bourboulia and Stetler-Stevenson, 2010; Brew and Nagase, 2010; Troeberg et al, 2009; Wei et al, 2005) For example, Wei et al. reported that mutations in the N-terminal region of TIMP-3 significantly impaired MMP inhibition, but not effects upon cytokine processing (ADAM dependent), implying that a domain outside of the N-terminal region is responsible for this biological activity.(Wei et al, 2005) Past studies of TIMP-3 gene deletion in mice demonstrated not only an acceleration of adverse myocardial remodeling, but this was also associated with increased cytokine expression, notably TNF, providing further evidence for the duality of function of TIMP-3. (Hammoud et al, 2011; Kandalam et al, 2010) Inhibition of the initial inflammatory/wound healing response following MI can cause detrimental effects on post-MI remodeling.(Lindsey and Zamilpa, 2012; Ma et al, 2013; Spinale, 2007) Thus, the attenuation of specific determinants of macrophage activation/polarization, such as MCP-1 and MIP-1A, which was achieved by F-TIMP-3 but not N-TIMP-3, may not necessarily be beneficial. The present study using high sensitivity troponin measurements identified an equivalent degree of initial myocardial injury in all groups, and indices of apoptosis shifted in all 3 groups at 14 days post-MI. F-TIMP-3 injections directionally reduced both Bax (pro-apoptotic) and BCL2 (anti-apoptotic) at 14 days post-MI and thus may have not altered the stoichiometric balance of this specific apoptotic cascade. Whether and to what degree TIMP-3

JPET Fast Forward. Published on September 21, 2020 as DOI: 10.1124/jpet.120.000047
This article has not been copyedited and formatted. The final version may differ from this version.

injections may influence myocardial viability pathways post-MI remains unclear. Furthermore, while the present study identified injections of the full-length TIMP-3 attenuated indices of inflammation post-MI at the transcriptional level, the downstream effects on inflammation remains to be fully explored.

The effects on post-MI remodeling achieved in the present study using local injection of TIMP-3 formulations appeared equivalent to that reported with systemic pharmacological MMP inhibition. (Awad et al, 2010; Bolz et al, 2016; Konstam et al, 2011; Ma et al, 2017; Webb et al, 2006; Weir et al, 2006; Zamilpa et al, 2011) While the regulation of MMP activity has been shown to be a relevant therapeutic target in a number of tissue remodeling processes such as cancer, rheumatoid, and cardiovascular disease, systemic delivery of pharmacological MMP inhibitors remains a significant challenge. (Dorman et al, 2010; Peterson, 2004) In terms of post-MI remodeling, a pharmacological MMP inhibitor was advanced to initial clinical trials. (Hudson et al, 2006) In an initial study utilizing a pharmacological MMP inhibitor in post-MI patients, a sub-optimal dosing schedule was utilized due to concerns regarding systemic effects and thus the likelihood of achieving local MMP inhibition was minimal. (Hudson et al, 2006; Spinale, 2007) There are inherent limitations of the present study that must be acknowledged. First, this study used a single time in the myocardial tissue that was quite short (days), and our initial injection studies demonstrated that only a small amount of the injected TIMP-3 formulation remained over a time course relevant to the present study period. The relative retention time of the N-TIMP-3 was shorter than the F-TIMP-3 and was likely due to the lower molecular weight of this truncated TIMP-3 molecule as well as the fact that ECM binding domains contained within the F-TIMP-3 molecule were absent. This laboratory reported the use of a slow release hydrogel construct (Eckhouse et al, 2014) that may improve localized release of TIMP-3 formulations. Finally, the present study utilized a coronary ligation approach in order to induce a reproducible and well defined MI region. (Eckhouse et al, 2014; Mukherjee et al, 2008) However, a more common clinical event is an ischemic episode followed by reperfusion in which the extent and type of inflammation and MMP activation may be quite different. Nevertheless, these proof of concept studies clearly demonstrate the feasibility and early efficacy of this therapeutic approach in terms of interrupting the course of adverse LV remodeling post-MI.

JPET Fast Forward. Published on September 21, 2020 as DOI: 10.1124/jpet.120.000047
This article has not been copyedited and formatted. The final version may differ from this version.

JPET Fast Forward. Published on September 21, 2020 as DOI: 10.1124/jpet.120.000047
This article has not been copyedited and formatted. The final version may differ from this version.

Conflict Statement[1]

JWO, SS, AK, and TL are employees of Amgen Inc. that manufacture drugs for a wide range of diseases, including cardiovascular disease. The other authors declare that they have no competing interests. The recombinant TIMP-3 formulations were furnished as an MTA from Amgen to FGS.

Author contributions.

Participated in Research Design: Lobb, Brower, Lee, Khakoo, Spinale
Conducted Experiments: Lobb, Doviak, Brower, Romito, Shuman, Freels, Zellars, Freeburg, Spinale
Contributed New Reagents or Analytical Tools: O'Neill, Smith, Lee, Khakoo
Performed Data Analysis: Doviak, Romito, Shuman, Freels, Zellars, Freeburg, Spinale
Wrote or Contributed to the Writing of the Manuscript: Lobb, Lee, Spinale

[1] This work was supported by the National Institute of Health grants HL111090 and HL113352, a Merit Award from the Veterans' Affairs Health Administration, and a basic research grant from Amgen, Inc.

JPET Fast Forward. Published on September 21, 2020 as DOI: 10.1124/jpet.120.000047
This article has not been copyedited and formatted. The final version may differ from this version.

References

Abbate A, Biondi-Zoccai GGL, Baldi A. (2002) Pathophysiologic role of myocardial apoptosis in post-infarction left ventricular remodeling. J Cell Physiol.193(2):145-53.

Awad AE, Kandalam V, Chakrabarti S, Wang X, Penninger JM, Davidge ST, Oudit GY, Kassiri Z. (2010) Tumor necrosis factor induces matrix metalloproteinases in cardiomyocytes and cardiofibroblasts differentially via superoxide production in a PI3Kgamma-dependent manner. Am J Physiol Cell Physiol. 298(3):C679-92.

Bolz M, Ruggli N, Borel N, Pluschke G, Ruf MT. (2016) Local Cellular Immune Responses and Pathogenesis of Buruli Ulcer Lesions in the Experimental Mycobacterium Ulcerans Pig Infection Model. PLoS Negl Trop Dis. 10(4):e0004678.

Bourboulia D, Stetler-Stevenson WG. (2010) Matrix metalloproteinases (MMPs) and tissue inhibitors of metalloproteinases (TIMPs): Positive and negative regulators in tumor cell adhesion. Semin Cancer Biol. 20:161-8.

Brew K, Nagase H. (2010) The tissue inhibitors of metalloproteinases (TIMPs): an ancient family with structural and functional diversity. Biochim Biophys Acta. 1803:55-71.

Colucci WS, Braunwald E. (2005) Pathophysiology of Heart Failure. Braunwald's Heart Disease. 7: 509-538.

Dewald O, Zymek P, Winkelmann K, Koerting A, Ren G, Abou-Khamis T, Michael LH, Rollins BJ, Entman ML, Frangogiannis NG. (2005) CCL2/Monocyte Chemoattractant Protein-1 regulates inflammatory responses critical to healing myocardial infarcts. Circ Res. 96:881-9.

Dixon JA, Spinale FG. (2009) Large animal models of heart failure: a critical link in the translation of basic science to clinical practice. Circ Heart Fail. 2:262-71.

Dormán G, Cseh S, Hajdú I, Barna L, Kónya D, Kupai K, Kovács L, Ferdinandy P. (2010) Matrix metalloproteinase inhibitors: a critical appraisal of design principles and proposed therapeutic utility. Drugs. 70:949-64.

Douglas DA, Shi YE, Sang QA. (1997) Computational sequence analysis of the tissue inhibitor of metalloproteinase family. J Protein Chem. 16:237-55.

Eckhouse SR, Purcell BP, Oelsen JM, Logdon CB, Rawls WF, Patel RK, Zellars KN, Stroud RE, Jones JA, Mukherjee R, Gorman JH III, Gorman RC, Black RA, Burdick JA, Spinale FG. (2014) Local hydrogel release of recombinant TIMP-3 attenuates adverse left ventricular remodeling after experimental myocardial infarction. Sci Transl Med. 6(223):223ra21.

Frangogiannis NG. (2012) Regulation of the inflammatory response in cardiac repair. Circ Res. 110:159-73.

Fu X, Khalil H, Kanisicak O, Boyer JG, Vagnozzi RJ, Maliken BD, Sargent MA, Prasad V,

Valiente-Alandi I, Blaxall BC, Molkentin JD. (2018) Specialized fibroblast differentiated states underlie scar formation in the infarcted mouse heart. J Clin Invest. 128(5):2127-2143.

Hammoud L, Burger DE, Lu X, Feng Q. Tissue inhibitor of metalloproteinase-3 inhibits neonatal mouse cardiomyocyte proliferation via EGFR/JNK/SP-1 signaling. (2009) Am J Physiol Cell Physiol. 296(4):C735-45.

Hammoud, L, Lu Xiangru, Feng Qingping. (2011) Deficiency in TIMP-3 increases cardiac rupture and mortality post-myocardial infarction via EGFR signaling: beneficial effects of cetuximab. Basic Res Cardiol. 106(3):459-71.

Heymans S, Luttun A, Nuyens D, Theilmeier G, Creemers E, Moons L, Dyspersin GD, Cleutjens JP, Shipley M, Angellilo A, Levi M, Nube O, Baker A, Keshet E, Lupu F, Herbert JM, Smits JF, Shapiro SD, Baes M, Borgers M, Collen D, Daemen MJ, and Carmeliet P. (1999) Inhibition of plasminogen activators or matrix metalloproteinases prevents cardiac rupture but impairs therapeutic angiogenesis and causes cardiac failure. Nat Med. 5: 1135-1142.

Hudson MP, Armstrong PW, Ruzyllo W, Brum J, Cusmano L, Krzeski P, Lyon R, Quinones M, Theroux P, Sydlowski D, Kim HE, Garcia MJ, Jaber WA, Weaver WD. (2006) Effects of selective matrix metalloproteinase inhibitor (PG-116800) to prevent ventricular remodeling after myocardial infarction: results of the PREMIER (Prevention of Myocardial Infarction Early Remodeling) trial. J Am Coll Cardiol. 48:15-20.

Kandalam V, Basu R, Abraham T, Wang X, Awad A, Wang W, Lopaschuk GD, Maeda N, Oudit GY, Kassiri Z. (2010) Early activation of matrix metalloproteinases underlies the exacerbated systolic and diastolic dysfunction in mice lacking TIMP3 following myocardial infarction. Am J Physiol Heart Circ Physiol. 299:H1012-23.

Kassiri Z, Defamie V, Hariri M, Oudit GY, Anthwal S, Dawood F, Liu P, Khokha R. (2009) Simultaneous transforming growth factor beta-tumor necrosis factor activation and cross-talk cause aberrant remodeling response and myocardial fibrosis in Timp3-deficient heart. J Biol Chem. 284(43):29893-904.

Khalil H, Kanisicak O, Prasad V, Correll RN, Fu X, Schips T, Vagnozzi RJ, Liu R, Huynh T, Lee S, Karch J, Molkentin JD. (2017) Fibroblast-specific TGF-β-Smad2/3 signaling underlies cardiac fibrosis. J Clin Invest. 127(10):3770-3783.

Konstam MA, Kramer DG, Patel AR, Maron MS, Udelson JE. (2011) Left ventricular remodeling in heart failure: current concepts in clinical significance and assessment. JACC Cardiovasc Imaging. 4:98-108.

Leco KJ, Khokha R, Pavloff N, Hawkes SP, and Edwards DR. (1994) Tissue inhibitor of metalloproteinases-3 (TIMP-3) is an extracellular matrix-associated protein with a distinctive pattern of expression in mouse cells and tissues. J Biol Chem 269: 9352-9360.

Lindsey ML, Gannon J, Aikawa M, Schoen FJ, Rabkin E, Lopresti-Morrow L, Crawford J, Black

S, Libby P, Mitchell PG, Lee RT. (2002) Selective matrix metalloproteinase inhibition reduces left ventricular remodeling but does not inhibit angiogenesis after myocardial infarction. Circulation. 105:753-758.

Lindsey ML, Zamilpa R. (2012) Temporal and spatial expression of matrix metalloproteinases and tissue inhibitors of metalloproteinases following myocardial infarction. Cardiovasc Ther. 30:31-41.

Lovelock JD, Baker AH, Gao F, Dong JF, Bergeron AL, McPheat W, Sivasubramanian N, Mann DL. (2005) Heterogeneous effects of tissue inhibitors of matrix metalloproteinases on cardiac fibroblasts. Am J Physiol Heart Circ Physiol. 288:H461-8.

Lu Y, Liu S, Zhang S, Cai G, Jiang H, Su H, Li X, Hong Q, Zhang X, Chen X. (2011) Tissue inhibitor of metalloproteinase-1 promotes NIH3T3 fibroblast proliferation by activating p-Akt and cell cycle progression. Mol Cells. 31:225-30.

Ma Y, Halade GV, Zhang J, Ramirez TA, Levin D, Voorhees A, Jin YF, Han HC, Manicone AM, Lindsey ML. (2013) Matrix metalloproteinase-28 deletion exacerbates cardiac dysfunction and rupture after myocardial infarction in mice by inhibiting M2 macrophage activation. Circ Res. 112(4):675-88

Ma Y, Iyer RP, Jung M, Czubryt MP, Lindsey ML. (2017) Cardiac Fibroblast Activation Post-Myocardial Infarction: Current Knowledge Gaps. Trends Pharmacol Sci. 38(5):448-458.

Melendez-Zajgla J, Del Pozo L, Ceballos G, Maldonado V. (2008) Tissue inhibitor of metalloproteinases-4. The road less traveled. Mol Cancer. 7:85.

Moore L, Fan D, Basu R, Kandalam V, Kassiri Z. (2012) Tissue inhibitor of metalloproteinases (TIMPs) in heart failure. Heart Fail Rev. 17(4-5):693-706.

Mukherjee R, Brinsa TA, Dowdy KB, Scott AA, Baskin JM, Deschamps AM, Lowry AS, Escobar GP, Lucas DG, Yarbrough WM, Zile MR, Spinale FG. (2003) Myocardial infarct expansion and matrix metalloproteinase inhibition. Circulation 107: 618-25.

Mukherjee R, Zavadzkas JA, Saunders SM, McLean JE, Jeffords LB, Stroud RE, Leone AM, Koval CN, Rivers WT, Basu S, Sheehy A, Michal G, Spinale FG. (2008) Targeted myocardial microinjections of a biocomposite material reduces infarct expansion in pigs. Ann Thorac Surg. 86:1268-76.

Peterson JT, Li H, Dillon L, Bryant JW. (2000) Evolution of matrix metalloprotease and tissue inhibitor expression during heart failure progression in the infarcted rat. Cardiovasc Res. 46:307-15.

Peterson JT. (2004) Matrix metalloproteinase inhibitor development and the remodeling of drug discovery. Heart Fail Rev. 9:63-79.

Shinde AV, Frangogiannis NG. (2014) Fibroblasts in myocardial infarction: a role in inflammation and repair. J Mol Cell Cardiol. 70:74-82.

Spinale FG, Koval CN, Deschamps AM, Stroud RE, Ikonomidis JS. (2008) Dynamic changes in matrix metalloproteinase activity within the human myocardial interstitium during ischemia reperfusion. Circulation. 118:S16-23.

Spinale FG. (2007) Myocardial matrix remodeling and the matrix metalloproteinases: influence on cardiac form and function. Physiol Rev. 87:1285-342.

Sutton MG, Sharpe N. (2000) Left ventricular remodeling after myocardial infarction: pathophysiology and therapy. Circulation. 101:2981-8.

Troeberg L, Fushimi K, Scilabra SD, Nakamura H, Dive V, Thøgersen IB, Enghild JJ, Nagase H. (2009) The C-terminal domains of ADAMTS-4 and ADAMTS-5 promote association with N-TIMP-3. Matrix Biol. 28:463-9.

Wang X, Morelli MB, Matarese A, Sardu C, Santulli G. (2020) Cardiomyocyte-derived exosomal microRNA-92a mediates post-ischemic myofibroblast activation both in vitro and ex vivo. ESC Heart Fail. 7(1):284-288.

Webb CS, Bonnema DD, Ahmed SH, Leonardi AH, McClure CD, Clark LL, Stroud RE, Corn WC, Finklea L, Zile MR, Spinale FG. (2006) Specific temporal profile of matrix metalloproteinase release occurs in patients following myocardial infarction: relation to left ventricular remodeling. Circulation. 114:1020-7.

Wei S, Kashiwagi M, Kota S, Xie Z, Nagase H, Brew K. (2005) Reactive site mutations in tissue inhibitor of metalloproteinase-3 disrupt inhibition of matrix metalloproteinases but not tumor necrosis factor-alpha-converting enzyme. J Biol Chem. 280:32877-82.

Weir RA, McMurray JJ, Velazquez EJ. (2006) Epidemiology of heart failure and left ventricular systolic dysfunction after acute myocardial infarction: prevalence, clinical characteristics, and prognostic importance. Am J Cardiol. 97:13F-25F.

Wilson EM, Moainie SL, Baskin JM, Lowry AS, Deschamps AM, Mukherjee R, Guy TS, St John-Sutton MG, Gorman JH 3rd, Edmunds LH Jr, Gorman RC, Spinale FG. (2003) Region- and type-specific induction of matrix metalloproteinases in post-myocardial infarction remodeling. Circulation. 107:2857-63.

Yang TT and Hawkes SP. (1992) Role of the 21-kDa protein TIMP-3 in oncogenic transformation of cultured chicken embryo fibroblasts. Proc Natl Acad Sci U S A 89: 10676-10680.

Yu WH, Yu S, Meng Q, Brew K, Woessner JF Jr. (2000) TIMP-3 binds to sulfated glycosaminoglycans of the extracellular matrix. J Biol Chem. 275:31226-32.

Zamilpa R, Kanakia R, Cigarroa J 4th, Dai Q, Escobar GP, Martinez H, Jimenez F, Ahuja SS, Lindsey ML. (2011) CC chemokine receptor 5 deletion impairs macrophage activation and induces adverse remodeling following myocardial infarction. Am J Physiol Heart Circ Physiol. 300(4):H1418-26.

Zile MR, Desantis SM, Baicu CF, Stroud RE, Thompson SB, McClure CD, Mehurg SM, Spinale FG. (2011) Plasma biomarkers that reflect determinants of matrix composition identify the presence of left ventricular hypertrophy and diastolic heart failure. Circ Heart Fail. 4:246-56.

JPET Fast Forward. Published on September 21, 2020 as DOI: 10.1124/jpet.120.000047
This article has not been copyedited and formatted. The final version may differ from this version.

Figure Legends

Figure 1. (A) Structure/sequence for the full length TIMP-3 (F-TIMP-3). The domain that comprises binding and inhibition of active MMPs is the N-terminus, and a truncated peptide containing this entire region was synthesized (N-TIMP-3). (B) Inhibitory profiles for both F-TIMP-3 and N-TIMP-3 were examined using an MMP fluorescent activity assay. The dashed lines reflect the respective effective inhibitory concentration (IC_{50}). (C) Schematic of 6 point injection site for the TIMP-3 formulations. (OM1/OM2:Obtuse Marginal Coronary Artery 1/2) (D) LV myocardial injections of fluorescently labelled F-TIMP-3 or N-TIMP-3 (5 mg) demonstrated localization in the targeted area (3, 5 days post injection) with computed retention time for each TIMP-3 shown.

Figure 2. (A) Experimental design for LV function and myocardial injection/sampling. (B) Representative LV short axis views (TOP) and 2D targeted M-Mode images (BOTTOM) at Baseline (pre-MI) and at 14 days post-MI for the 3 groups. LV volumetric measurements were computed using LV long axis as well as short axis images. These echocardiograms exemplify the degree of LV dilation and loss of LV posterior free wall (LVFW) motion as well as wall thinning at 14 days post-MI. In both TIMP-3 injection groups, the magnitude of LV dilation and LVFW wall thinning were attenuated. Summary results for LV geometry and function are in Figure 3. EDD- LV end-diastolic dimension.

Figure 3. Plasma troponin-I levels were determined prior to MI induction (Baseline) at 24 and 72 hours post-MI induction, and at terminal study on post-MI day 14 in pigs randomized to the 3 treatment groups. Plasma troponin-I levels were near non-detectable levels at Baseline, spiked at 24 hours post-MI, and had returned to within Baseline ranges by 3 and 14 days post-MI in all groups. The inset panel presents the plasma troponin-I levels at 24 hours post-MI for all groups, and while increased from Baseline, were equivalent (ND - no significant difference). LV end-diastolic volume increased as a function of time post-MI but was reduced at later time points in both TIMP-3 formulation groups. These changes were paralleled by an improvement in LV ejection fraction and wall thickness (at MI region) in both TIMP-3 formulation groups. Additional indices of post-MI remodeling, as reflected by left atrial geometry (area) and filling pressure (pulmonary capillary wedge pressure), were reduced at later post-MI time points in

both TIMP-3 formulation groups. (*p<0.05 vs baseline values, +p<0.05 vs MI/saline; determined by post-hoc adjusted pairwise comparisons, LSD test. Sample sizes: MI/saline n=9, MI/F-TIMP-3 n=8, MI/N-TIMP-3 n=9)

Figure 4. A pattern of expression emerged whereby mRNA levels for MMPs and TIMPs were increased in the MI/saline and MI/N-TIMP-3 groups and reduced in the MI/F-TIMP-3 group. Of note, relative TIMP-3 mRNA levels were increased to the greatest degree in the MI/N-TIMP-3 group. (*p<0.05 vs control values, +p<0.05 vs MI/saline; #p<0.05 vs MI/F-TIMP-3, determined by non-parametric Wilcoxon test. Sample sizes: MI/saline n=9, MI/F-TIMP-3 n=8, MI/N-TIMP-3 n=9, Referent Control n=5)

Figure 5. Relative fibrillar collagen mRNA levels (collagen type I (COL1A1) and collagen type III (COL3A1)) increased post-MI in all groups compared to referent controls, but relative values were lower in the MI/F-TIMP-3 group. Representative mRNA levels from the cytokines and chemokines within the MI regions revealed a robust increase compared to referent controls with similar values between the MI/saline and MI/N-TIMP-3 groups. However, TNF, MCP1, and MIP1A were significantly lower in the MI/F-TIMP-3 group. Using an expanded cytokine array panel (Supplemental Table 2), a number of cytokines were increased post-MI, such as CCR-2 and IL-10, were reduced in the MI/F-TIMP-3 group, and were equivalent or increased from post-MI values in the MI/N-TIMP-3 group. (*p<0.05 vs control values, +p<0.05 vs MI/saline; #p<0.05 vs MI/F-TIMP-3, determined by LSD test. Sample sizes: MI/saline n=9, MI/F-TIMP-3 n=8, MI/N-TIMP-3 n=9, Referent Control n=5)

Figure 6. Targeted PCR measurements of determinants of apoptosis, BAX and BCL2 both increased in the MI/saline and MI/N-TIMP-3 groups and reduced in the MI/F-TIMP-3 group within the MI region. (*p<0.05 vs control values, +p<0.05 vs MI/saline; #p<0.05 vs MI/F-TIMP-3, determined by non-parametric Wilcoxon test. Sample sizes: MI/saline n=9, MI/F-TIMP-3 n=8, MI/N-TIMP-3 n=9, Referent Control n=5)

Figure 7. (A) In addition to targeted PCR cytokine measurements, a full cytokine porcine PCR array was utilized (Supplemental Table 2), which contained 84 unique cytokines and

JPET Fast Forward. Published on September 21, 2020 as DOI: 10.1124/jpet.120.000047
This article has not been copyedited and formatted. The final version may differ from this version.

chemokines. The composite values for all of these measurements are shown here whereby the ANOVA identified a significant overall treatment effect and pairwise comparisons revealed overall cytokine induction in the MI/saline and MI/N-TIMP-3 groups and lower values in the MI/F-TIMP-3 group. The composite cytokine value was the highest in the MI/N-TIMP-3 group. (B) Total MMP activity was determined in LV homogenates taken from the MI region and was increased within the MI region in all groups. (C) MT1-MMP (MMP-14) activity was also determined and revealed a similar pattern to that of total MMP activity. (*p<0.05 vs control values, +p<0.05 vs MI/saline; #p<0.05 vs MI/F-TIMP-3, determined by LSD test. Sample sizes: MI/saline n=9, MI/F-TIMP-3 n=8, MI/N-TIMP-3 n=9, Referent Control n=5)

Figure 8. (TOP) H&E sections revealed a loss of cardiac myocytes within the MI region accompanied by replacement fibrosis and the presence of inflammatory cells. PSR stained sections revealed clear bands of fibrillar collagen within the MI region. SMA staining of the MI region was robustly increased in all groups but appeared reduced in the F-TIMP-3 group. Macrophage staining (IBA antibody) revealed a minimal positive signal in the referent normal samples with a robust increase in all MI sections. (Original magnification 40X, bars=100 um). (BOTTOM) Relative collagen content was increased in the MI and remote regions in all treatment groups when compared to referent normal values. Quantitative analysis revealed a robust increase within the MI region for SMA and IBA, which remained elevated in both TIMP-3 groups. However, SMA levels within the MI region were lower in the MI/F-TIMP-3 group. Due to the nominal IBA staining in the remote regions, the quantitative results are not shown. However, representative histological sections for the remote region are provided in Supplemental Figure 1. (*p<0.05 vs control values, +p<0.05 vs MI/saline; #p<0.05 vs MI/F-TIMP-3, determined by LSD test. Sample sizes: MI/saline n=9, MI/F-TIMP-3 n=8, MI/N-TIMP-3 n=9, Referent Control n=5)

Figure 1.

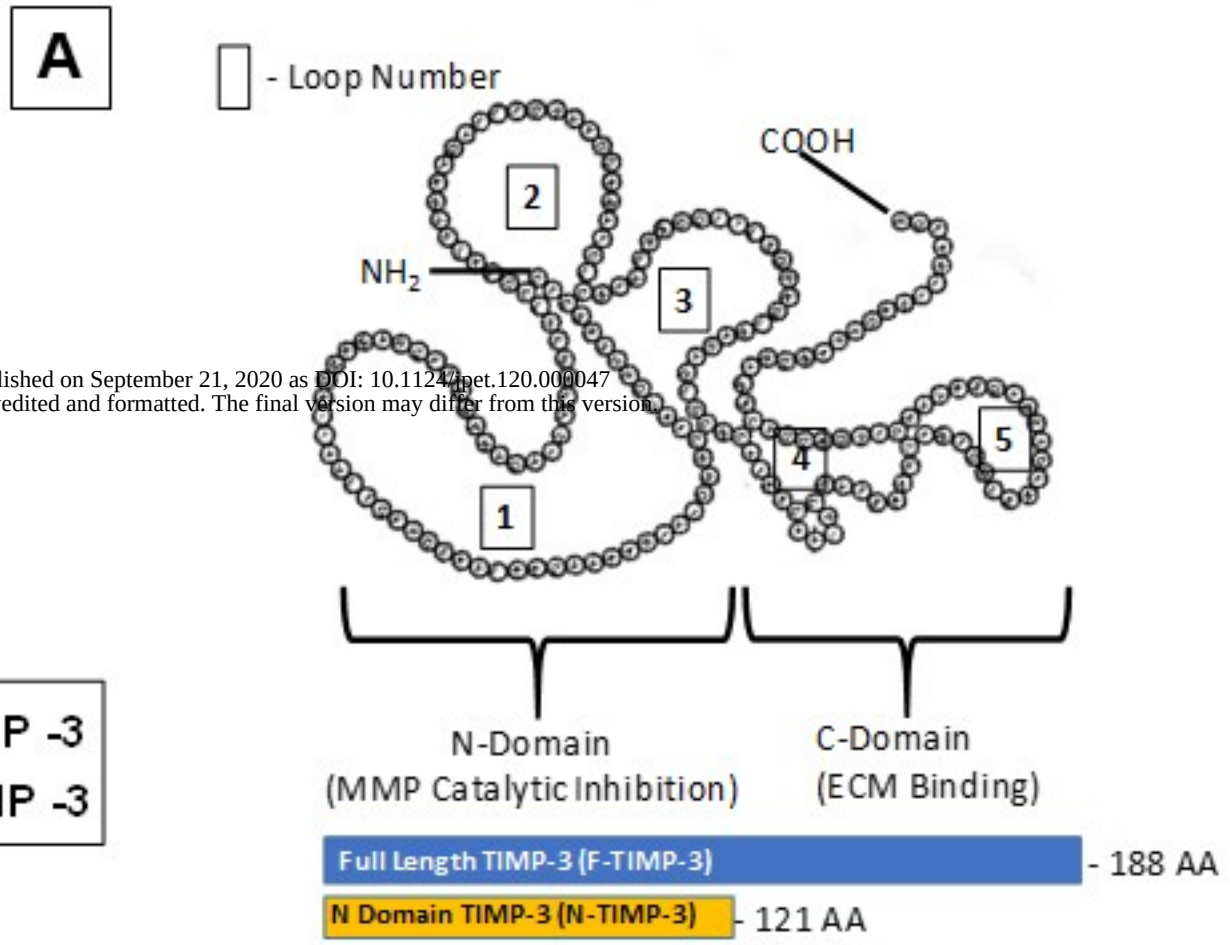

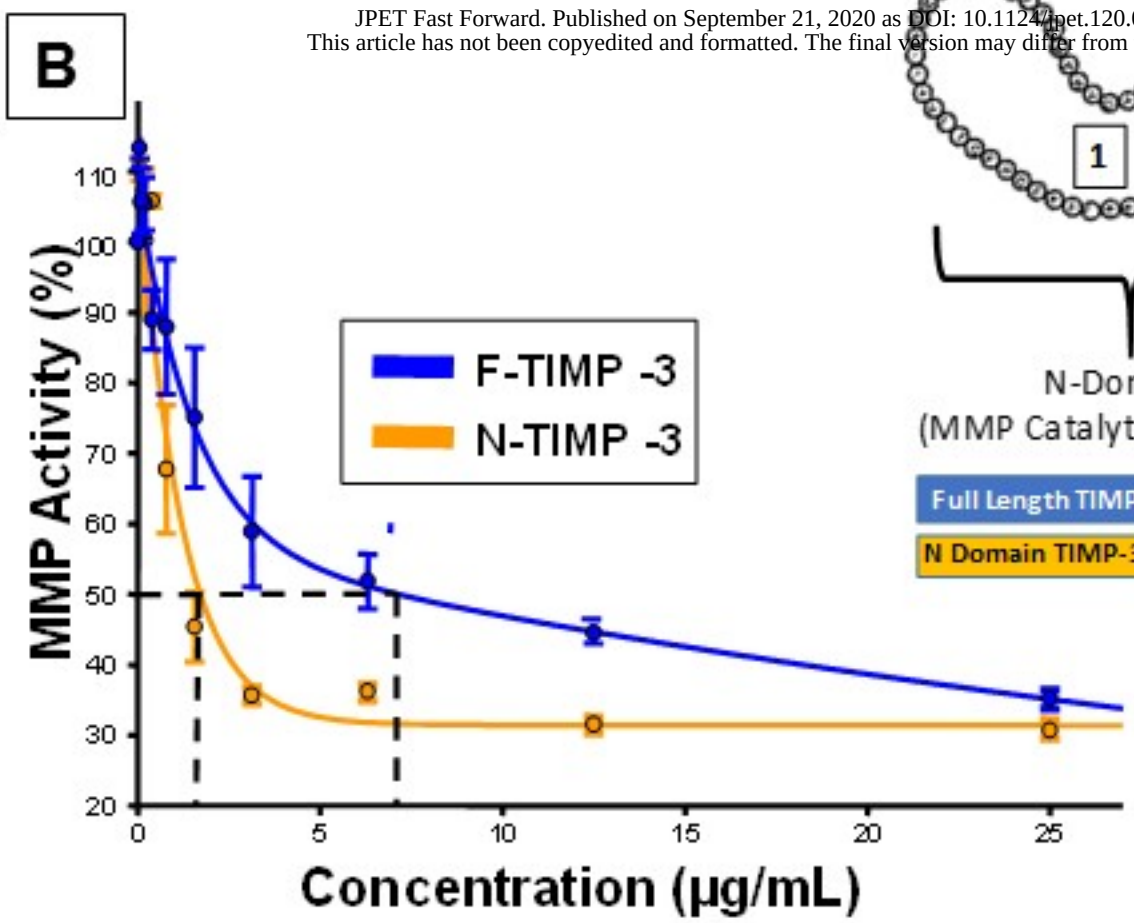

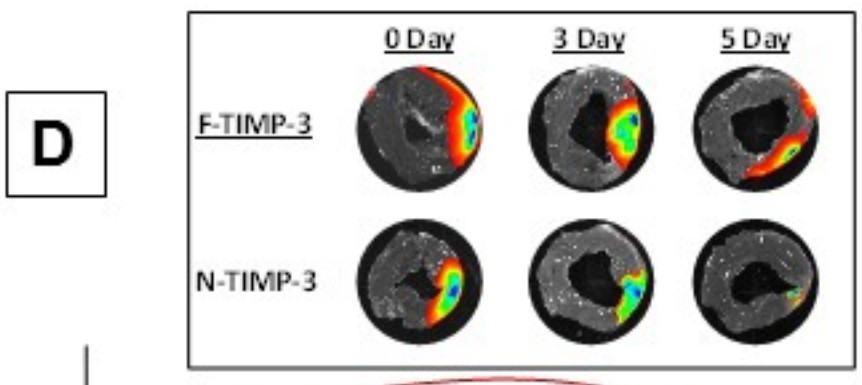

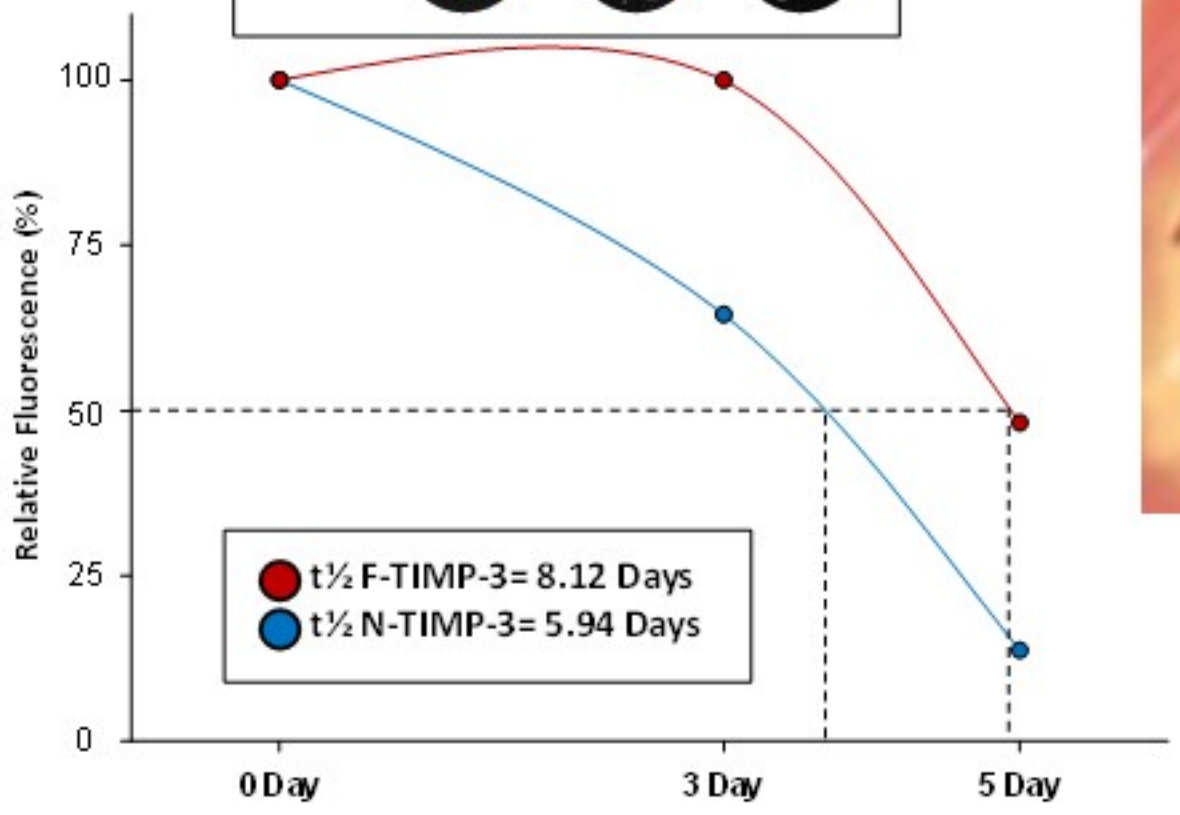

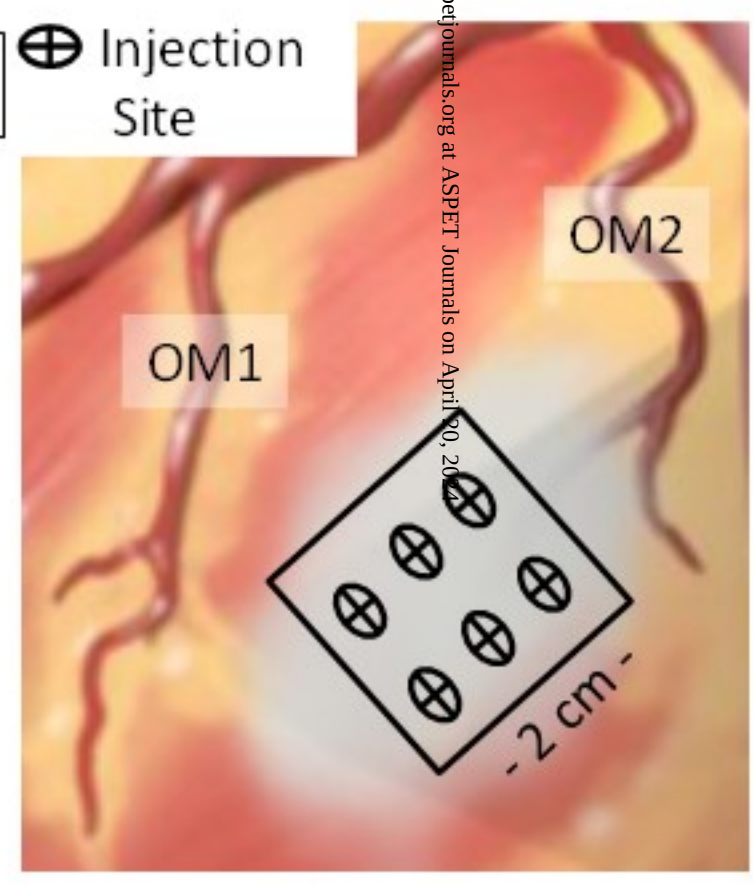

Figure 2.

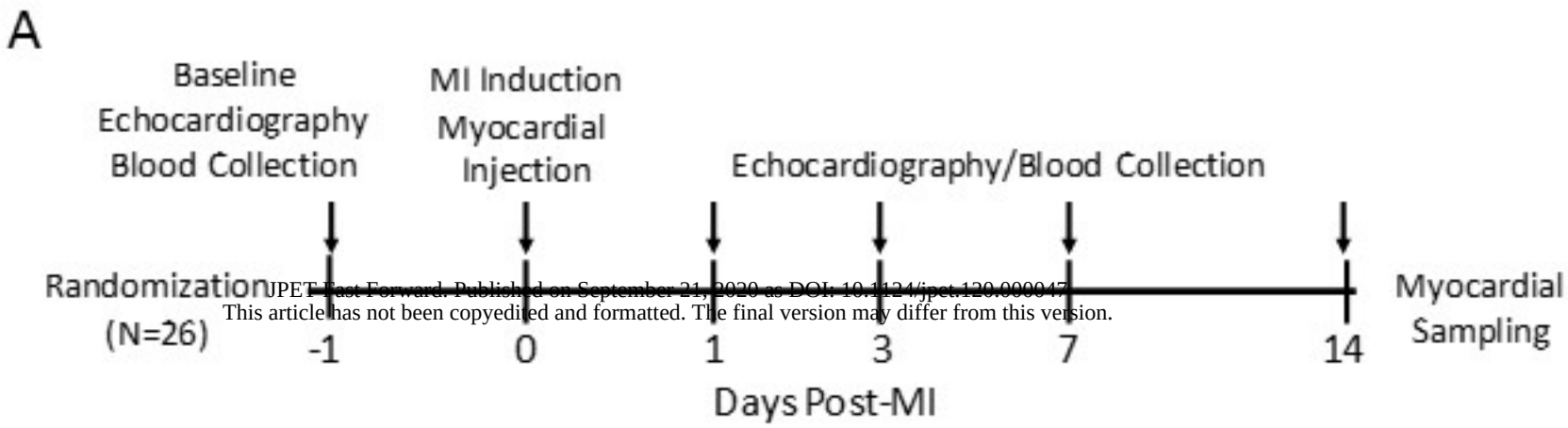

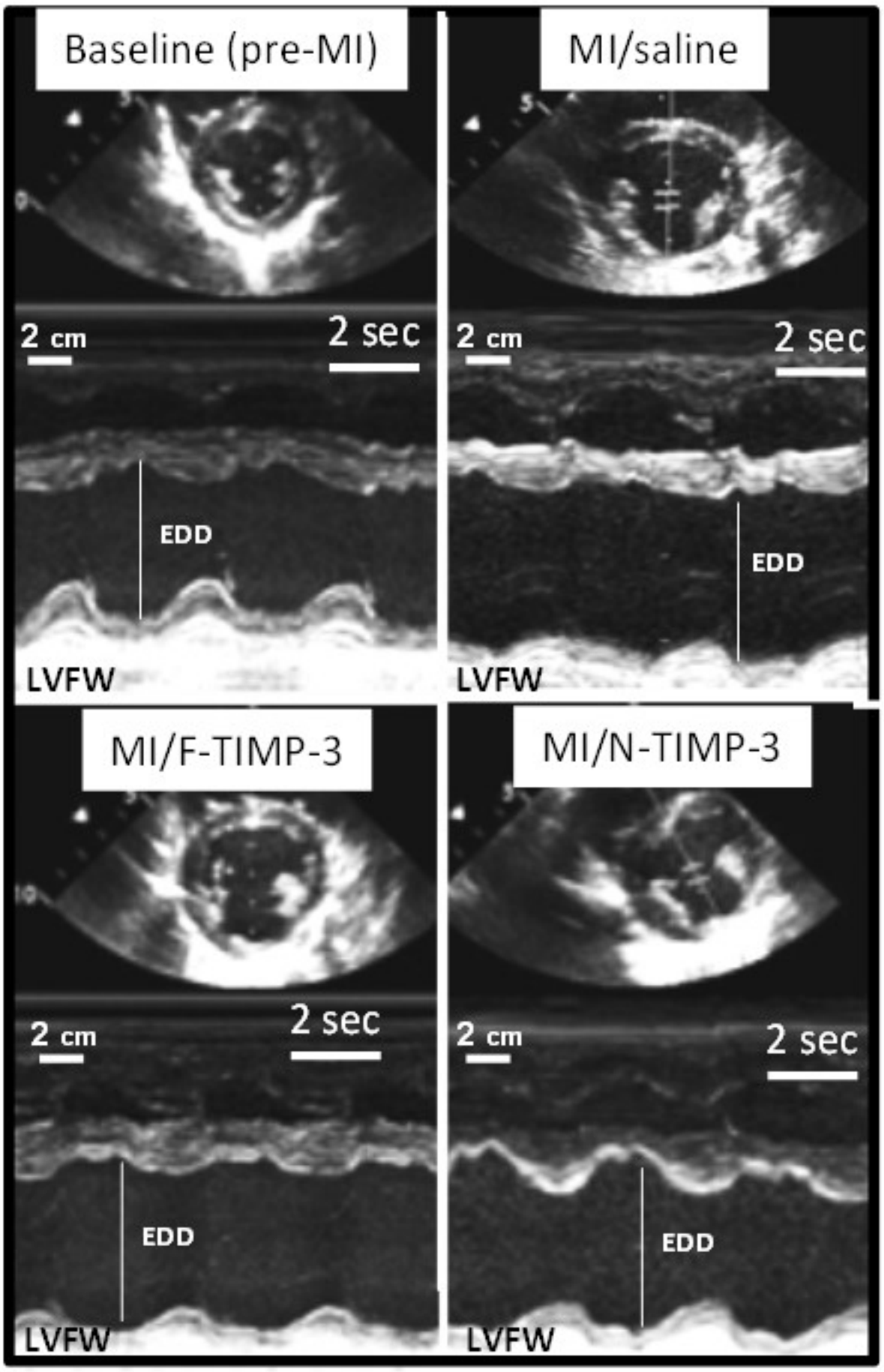

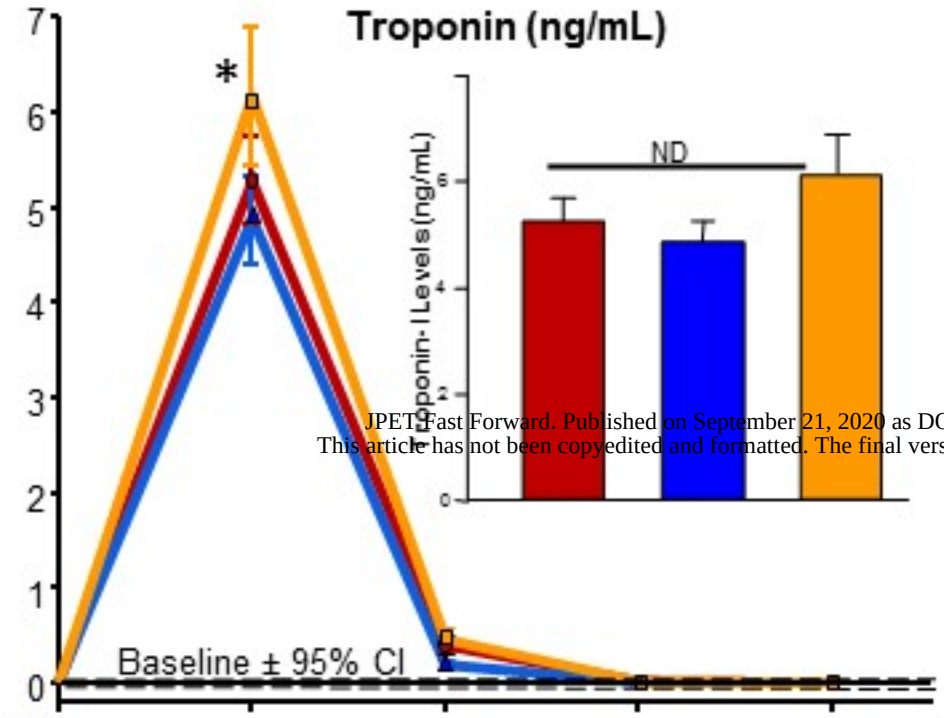

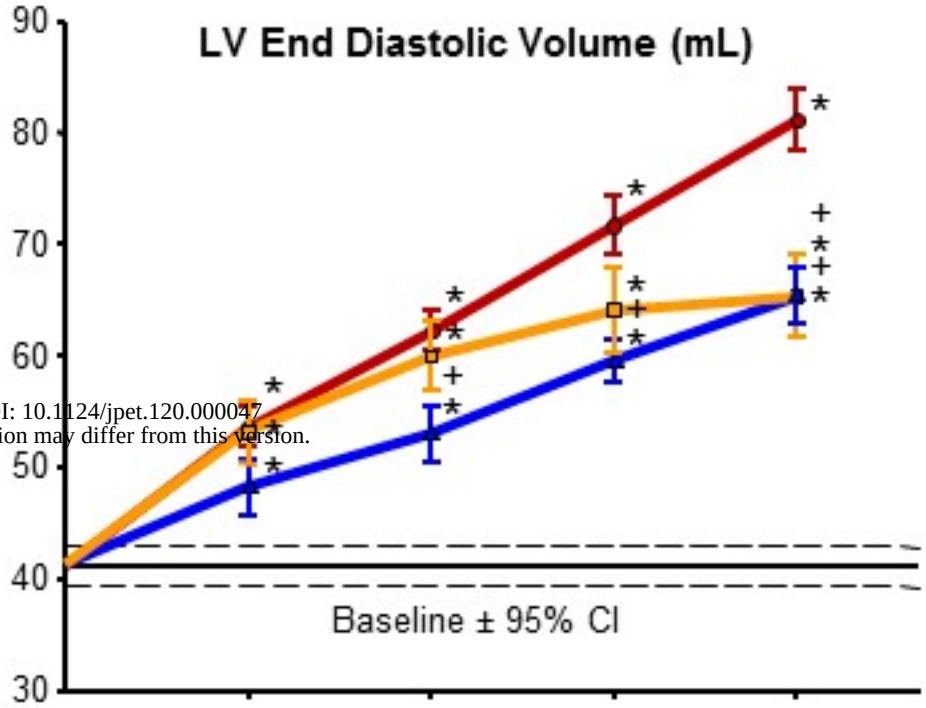

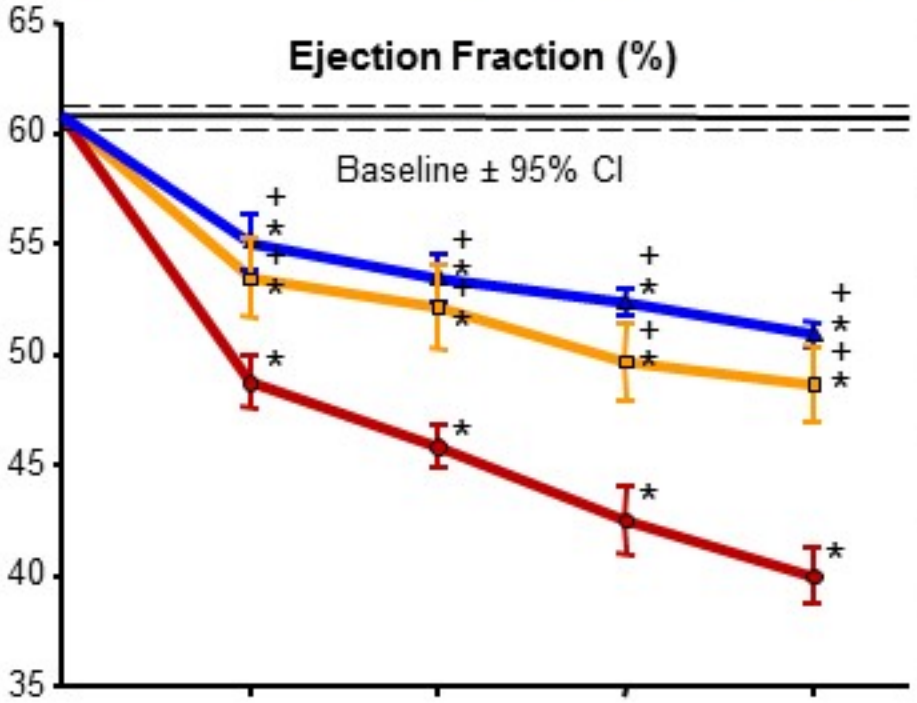

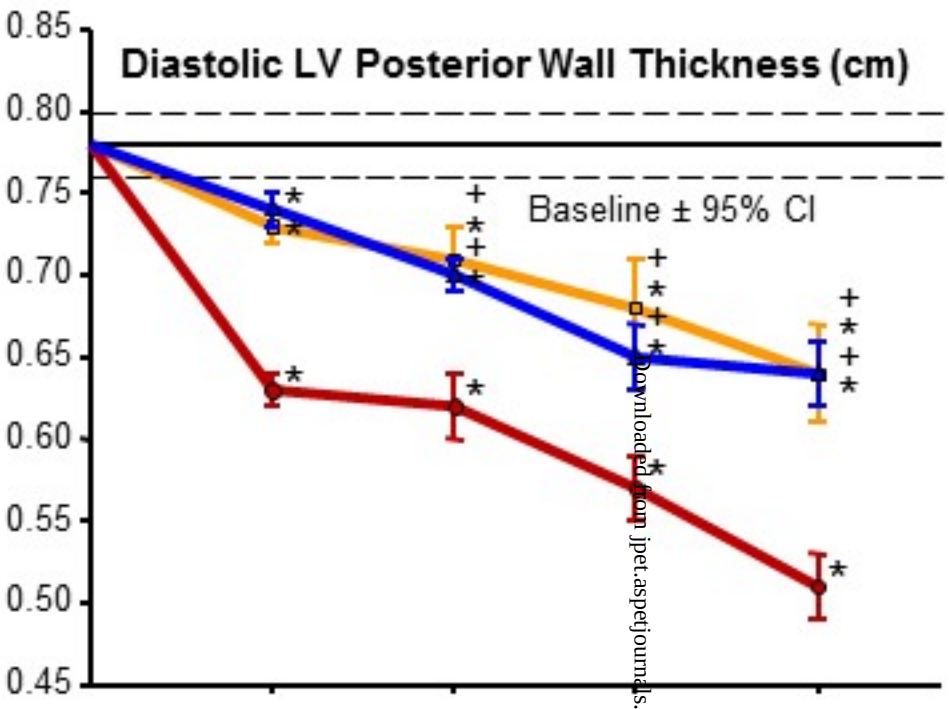

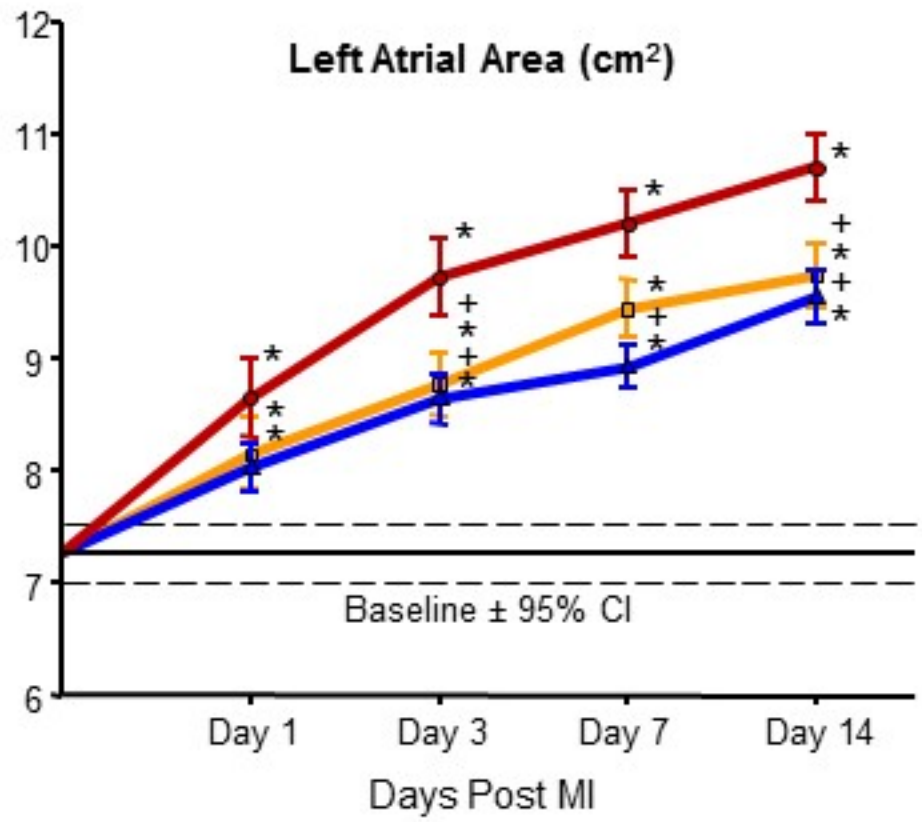

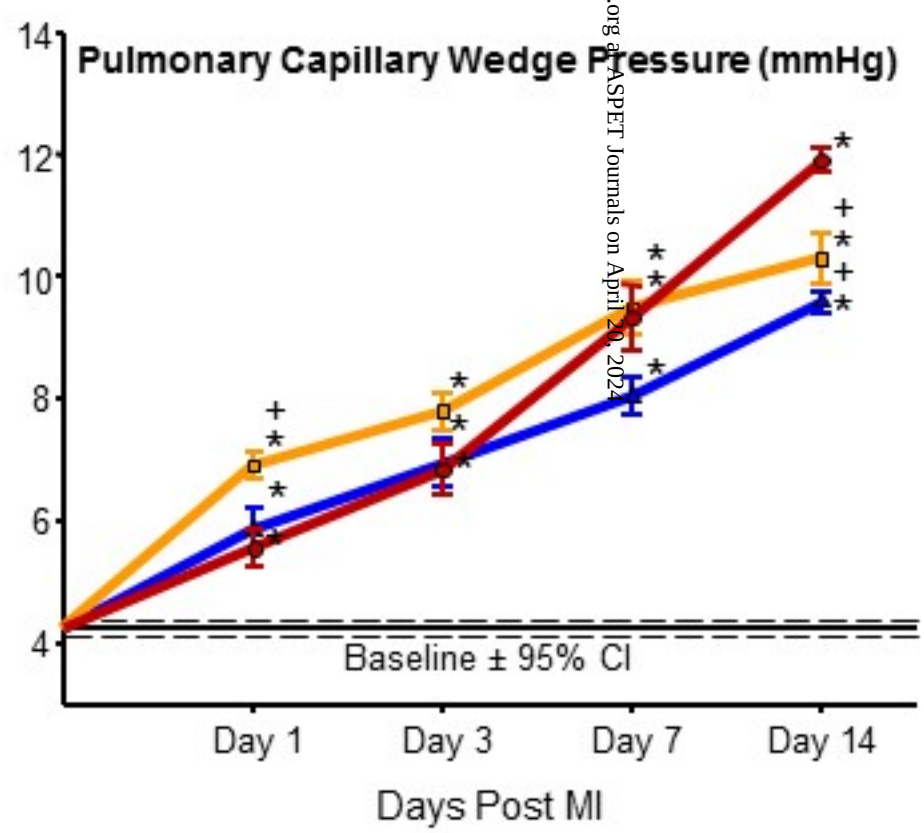

MI/saline
MI/F-TIMP-3
MI/N-TIMP-3

Figure 3.

JPET Fast Forward. Published on September 21, 2020 as DOI: 10.1124/jpet.120.000047
This article has not been copyedited and formatted. The final version may differ from this version.

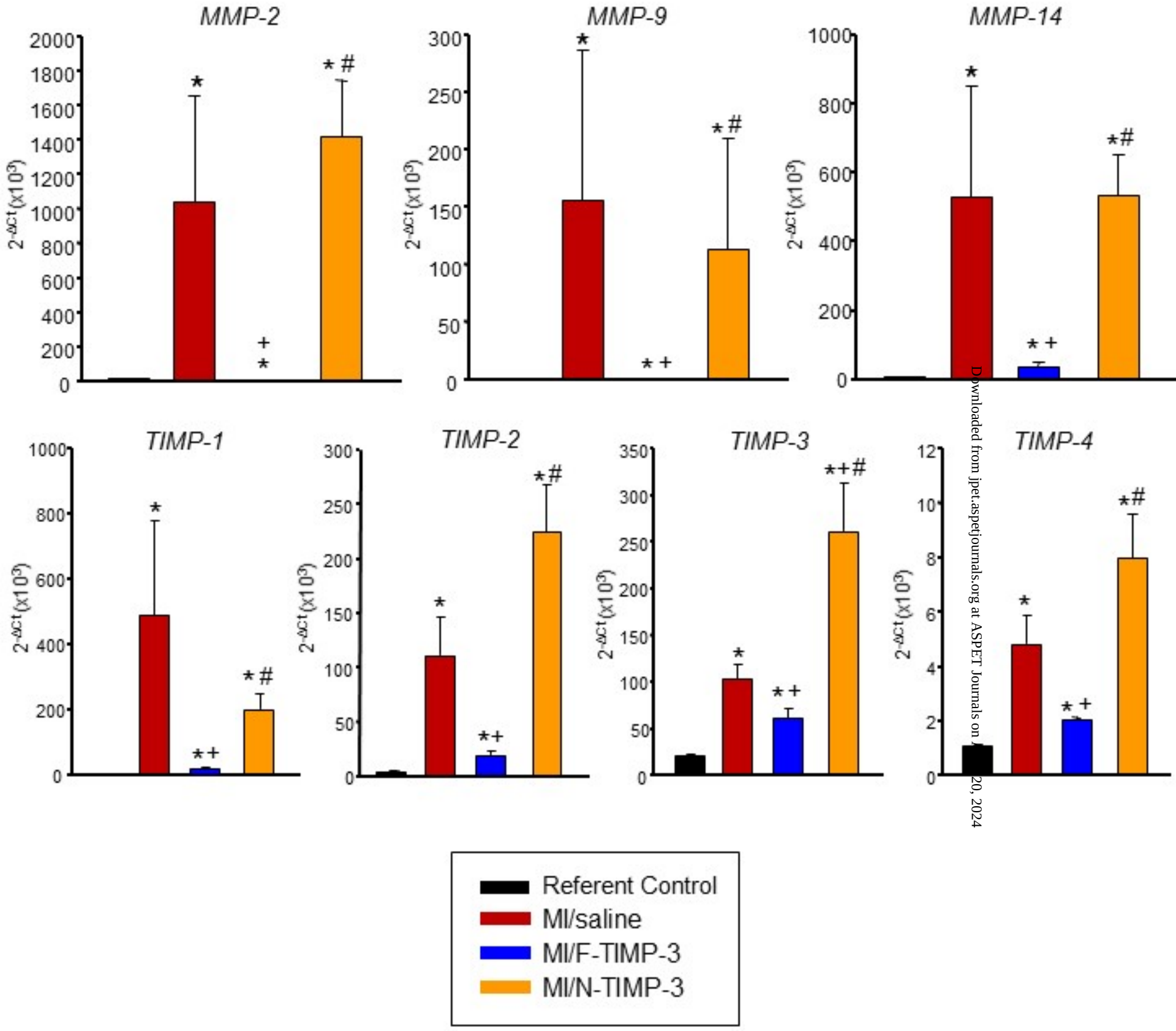

Figure 4.

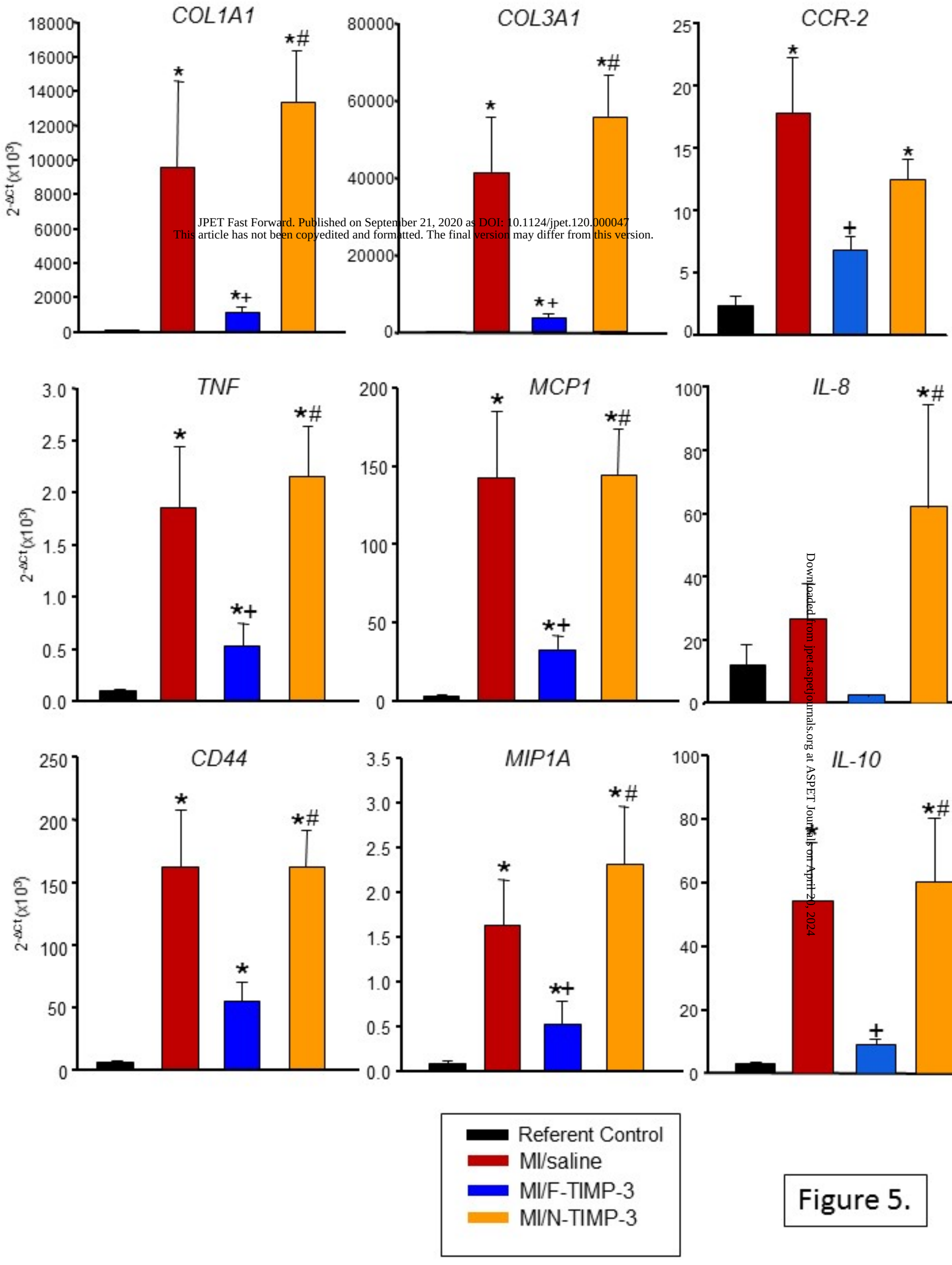

Figure 5.

Figure 6.

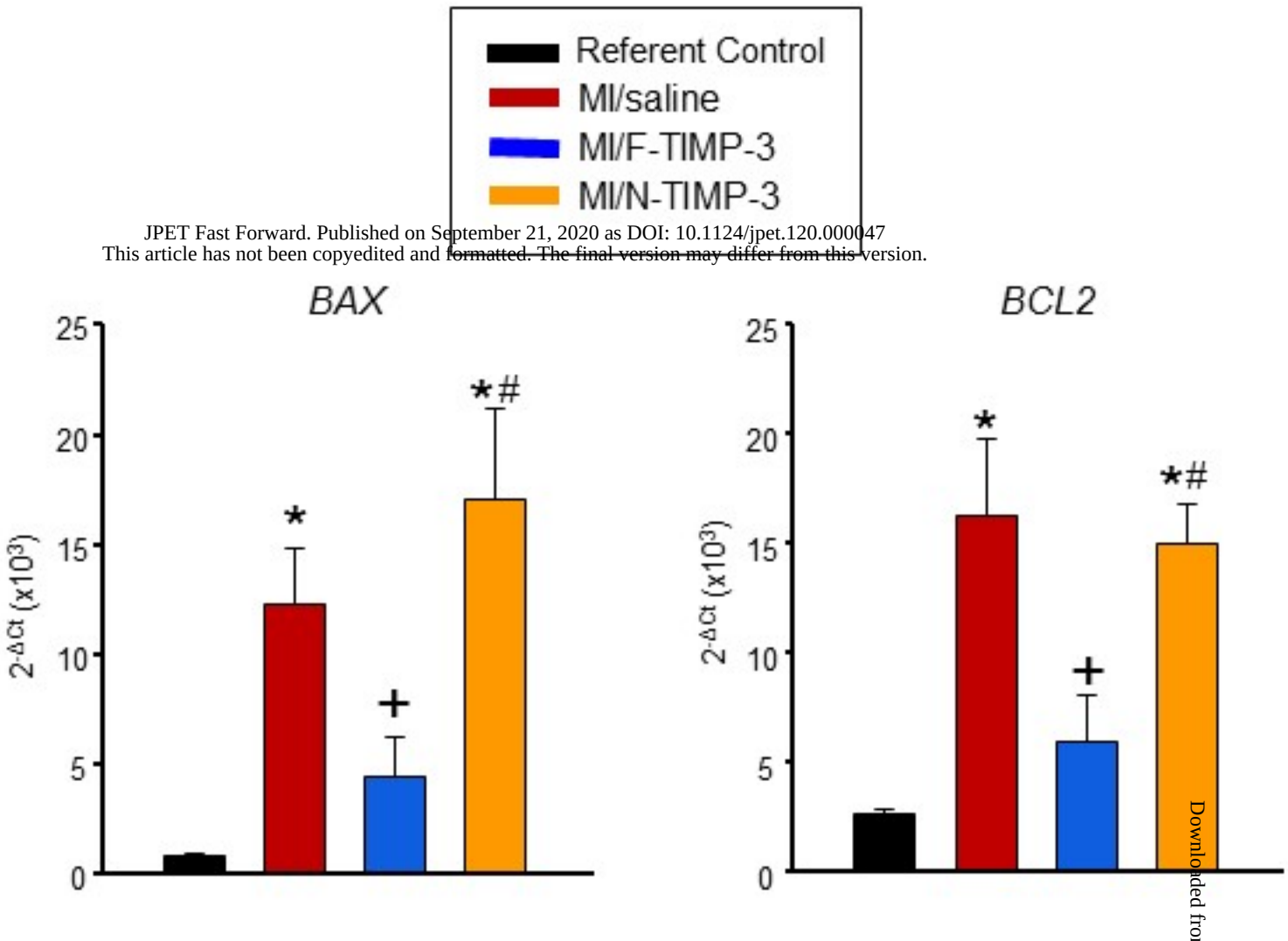

JPET Fast Forward. Published on September 21, 2020 as DOI: 10.1124/jpet.120.000047
This article has not been copyedited and formatted. The final version may differ from this version.

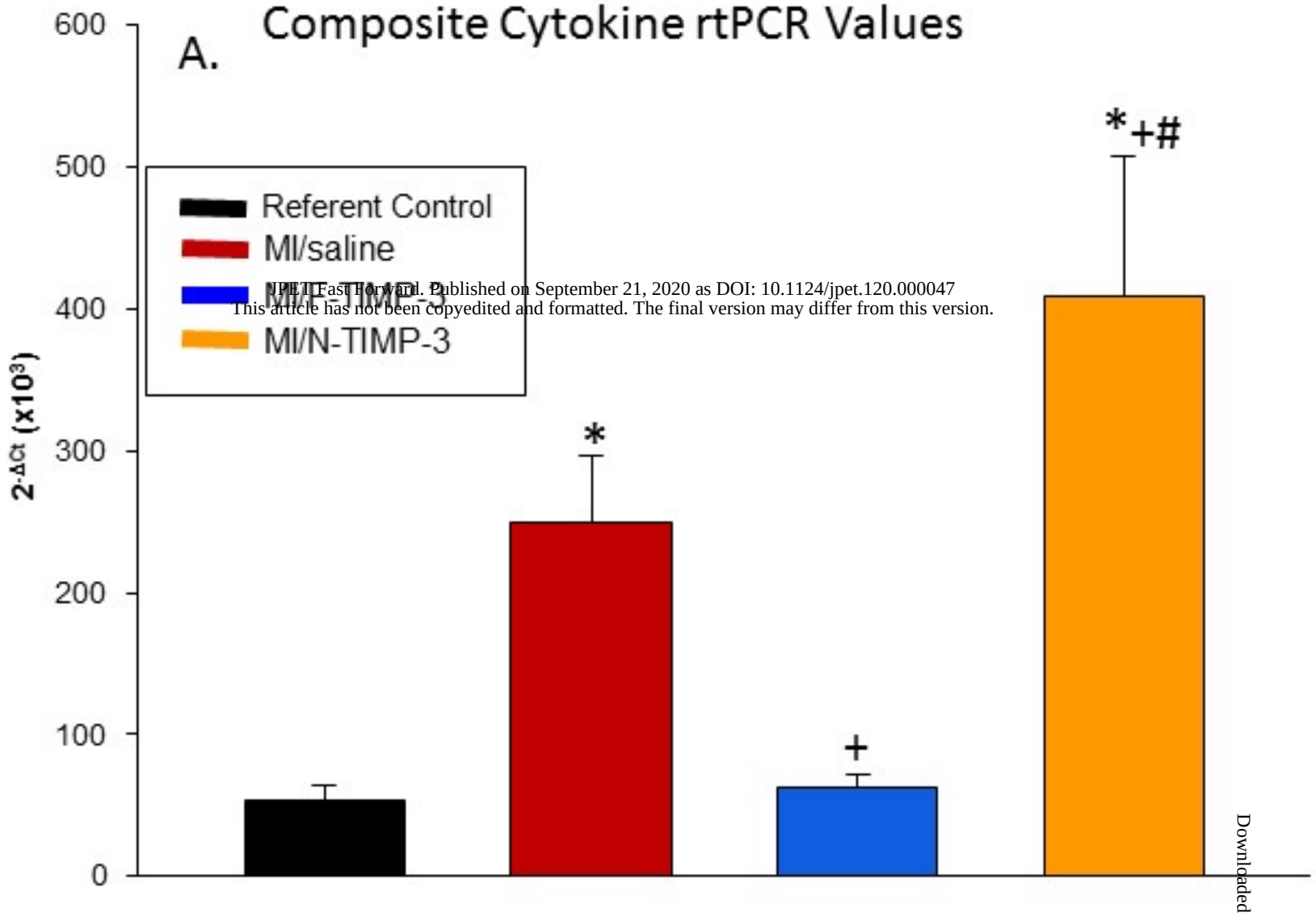

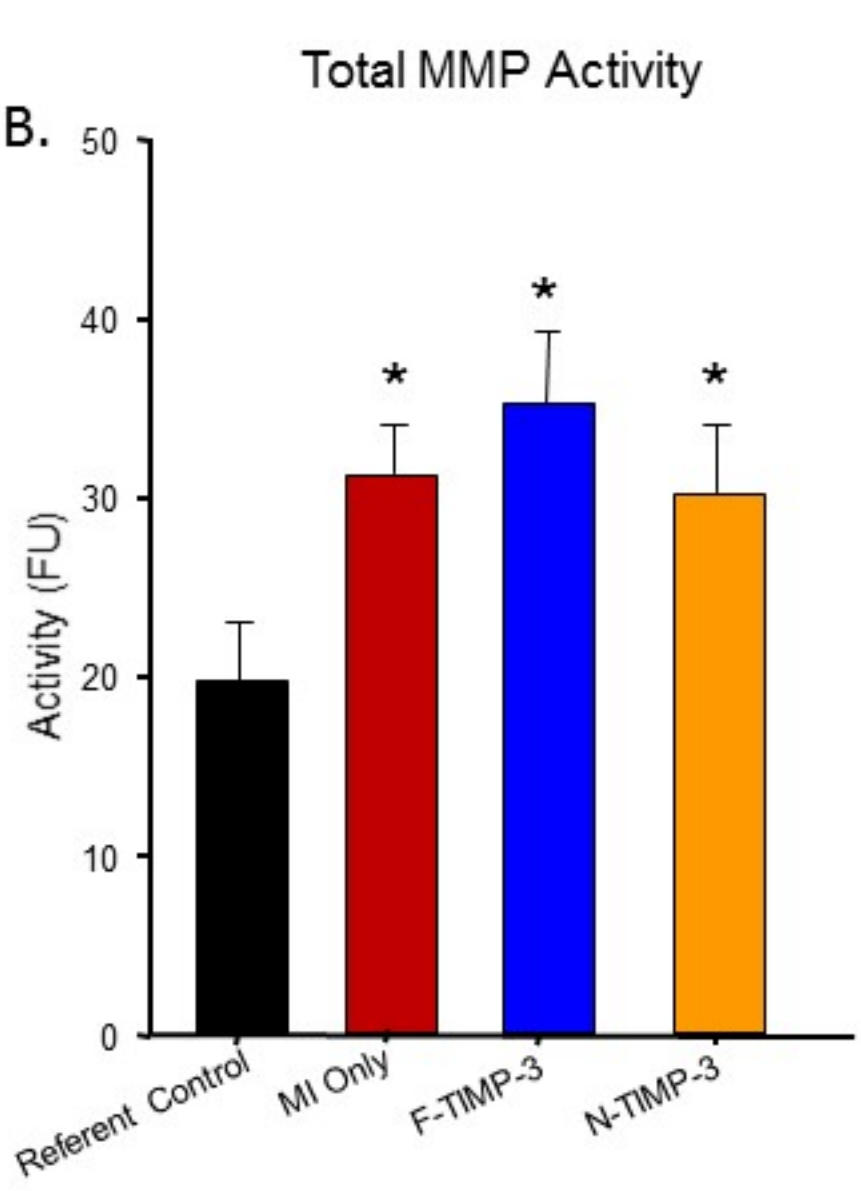

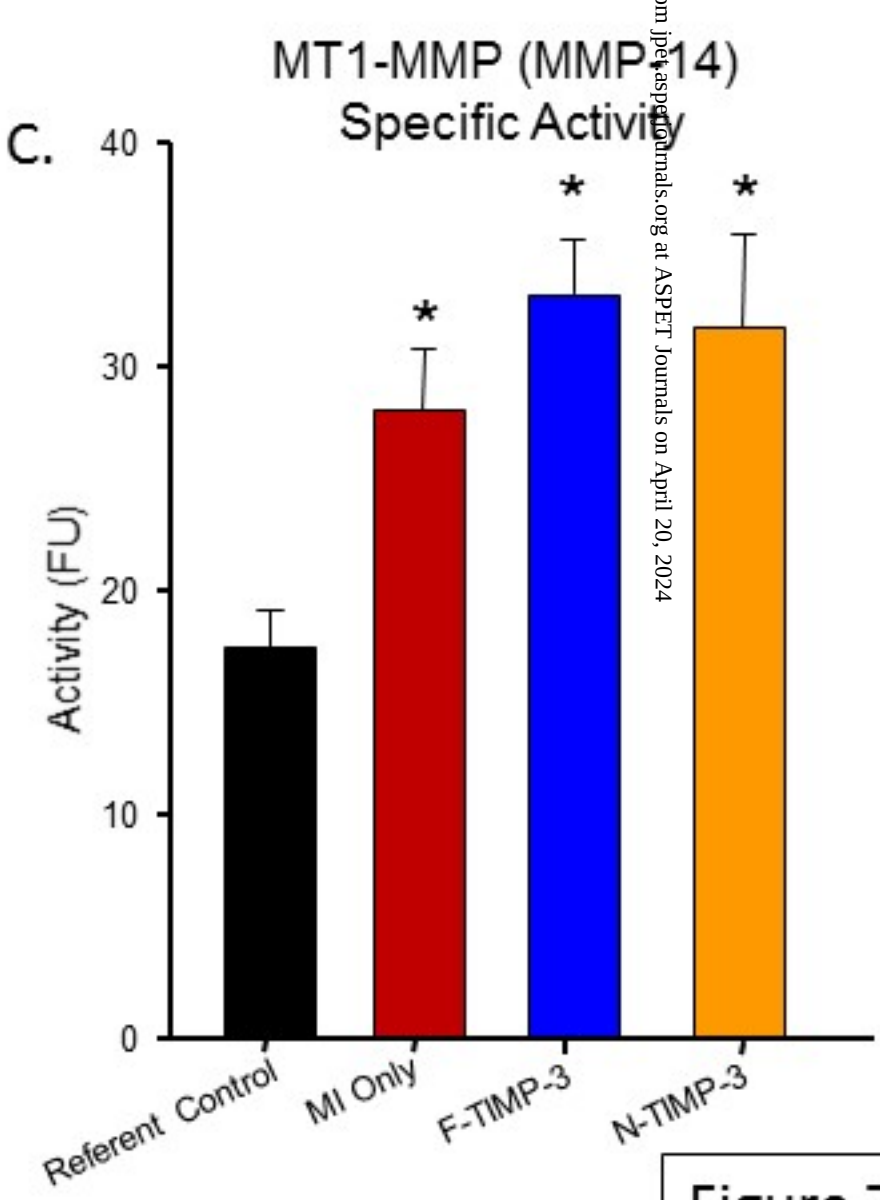

Figure 7.

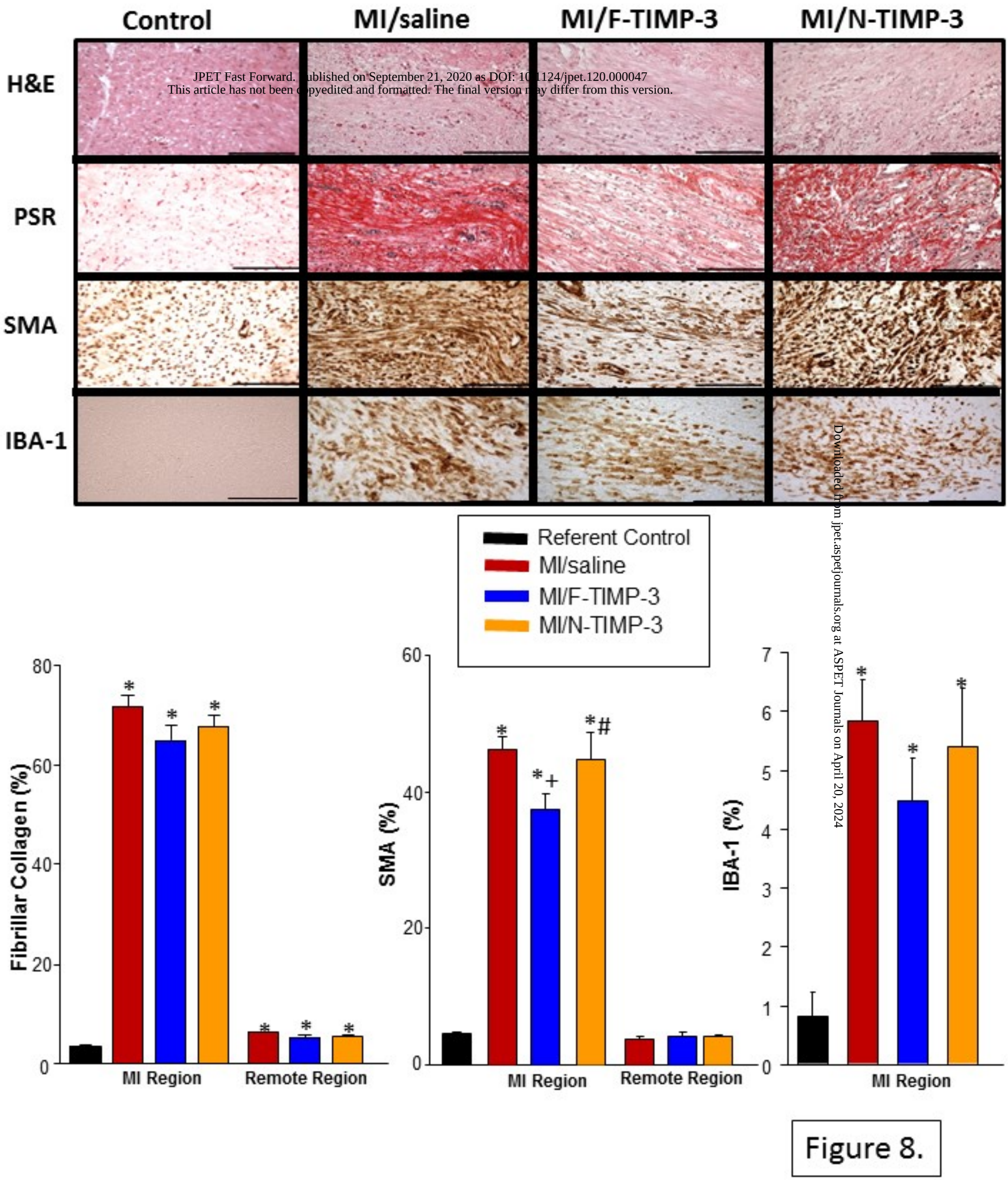

Figure 8.

JPET-AR-2020-000047

Targeted Injection of a Truncated Form of Tissue Inhibitor of Metalloproteinase 3 Alters Post-MI Remodeling

Running Title: TIMP-3 domains and post-MI remodeling

David C. Lobb, PhD[+], Heather Doviak, BS[+], Gregory L. Brower, PhD[+], Eva Romito, PhD[+], Jason W. O'Neill, PhD[§], Stephen Smith, PhD[§], James A. Shuman, MD[+], Parker D. Freels, MD[+], Kia N. Zellars, BS[+], Lisa A. Freeburg, BS[+], Aarif Y. Khakoo, MD[§], TaeWeon Lee, PhD[§], Francis G. Spinale, MD, PhD[+]

[+]Cardiovascular Translational Research Center, University of South Carolina School of Medicine and the WJB Dorn Veteran Affairs Medical Center, Columbia, SC; [§] Amgen, Metabolic Disorders, South San Francisco, CA

Supplement Table 1. Porcine Specific PCR Array Utilized in Post-MI Studies

	UniGene	GenBank #
Matrix Metalloproteinases (MMPs)		
MMP-2	Ssc. 5713	NM_214192
MMP-9	PPS01420	NM_001038004
MMP-13	Ssc. 16053	XM_003129808
MMP-14	Ssc. 734	NM_214239
Tissue Inhibitor of MMPs (TIMPs)		
TIMP1	Ssc. 11784	NM_213857
TIMP2	Ssc. 57257	NM_001145985
TIMP3	Ssc. 16028	XM_003126073

TIMP4	Ssc. 16027	XM_3358524
Fibrillar Collagen		
COL1A1	Ssc.55931	XM_003483014
COL3A1	Ssc. 24309	NM_001243297
Cytokines		
TNF	PPS00426	NM_214022
MCP-1	PPS00734	NM_214214
CD-44	PPS15136	XM_003122866
MIP-1a	Ssc. 24309	NM_001243297
Apoptosis		
BAX	Ssc. 23470	XM_003127290.2
BCL-2	Ssc. 53633	XM_003121700.4

COL1A1 – Collagen, Type I, Alpha 1
COL3A1 – Collagen, Type III, Alpha 1
TNF **–** Tumor Necrosis Factor Alpha
MCP-1 **–** Monocyte chemoattractant protein-1; Chemokine Ligand 2
MIP-1a **–** Macrophage Inflammatory Protein-1 alpha; Chemokine ligand 3
BAX- BCL2- associated X protein
BCL2- B-cell lymphoma 2

Targeted Injection of a Truncated Form of Tissue Inhibitor of Metalloproteinase 3 Alters Post-MI Remodeling

Running Title: TIMP-3 domains and post-MI remodeling

David C. Lobb, PhD[+], Heather Doviak, BS[+], Gregory L. Brower, PhD[+], Eva Romito, PhD[+], Jason W. O'Neill, PhD[§], Stephen Smith, PhD[§], James A. Shuman, MD[+], Parker D. Freels, MD[+], Kia N. Zellars, BS[+], Lisa A. Freeburg, BS[+], Aarif Y. Khakoo, MD[§], TaeWeon Lee, PhD[§], Francis G. Spinale, MD, PhD[+]

[+]Cardiovascular Translational Research Center, University of South Carolina School of Medicine and the WJB Dorn Veteran Affairs Medical Center, Columbia, SC; [§] Amgen, Metabolic Disorders, South San Francisco, CA

Supplemental Table 2. Porcine Specific Cytokine PCR Array

UniGene	GenBank	Symbol	Description
Ssc.56768	NM_001114283	AIMP1	Aminoacyl tRNA synthetase complex-interacting multifunctional protein 1
Ssc.4190	NM_001195399	BMP2	Bone morphogenetic protein 2
Ssc.21108	NM_001001646	C5	Complement component 5
Ssc.78517	NM_001166491	CCL1	Chemokine (C-C motif) ligand 1
Ssc.42664	NM_001256147	CCL17	Chemokine ligand 17-like protein
Ssc.657	NM_214214	CCL2	Chemokine (C-C motif) ligand 2
Ssc.42745	NM_001024589	CCL20	Chemokine (C-C motif) ligand 20
Ssc.18613	NM_001005151	CCL21	Chemokine (C-C motif) ligand 21
Ssc.48467	NM_001256776	CCL22	C-C motif chemokine 22-like
Ssc.43937	NM_001009579	CCL3L1	Chemokine (C-C motif) ligand 3-like 1
Ssc.23797	NM_213779	CCL4	Chemokine (C-C motif) ligand 4
Ssc.22030	NM_001129946	CCL5	Chemokine (C-C motif) ligand 5
Ssc.9957	NM_001164515	CCL8	Chemokine (C-C motif) ligand 8
Ssc.18359	NM_001001621	CCR1	Chemokine (C-C motif) receptor 1
Ssc.42655	NM_001044563	CCR10	Chemokine (C-C motif) receptor 10
Ssc.26329	NM_001001619	CCR2	Chemokine (C-C motif) receptor 2
Ssc.19054	NM_001001620	CCR3	Chemokine (C-C motif) receptor 3
N/A	XM_003361791	CCR4	Chemokine (C-C motif) receptor 4
Ssc.26328	NM_001001618	CCR5	Chemokine (C-C motif) receptor 5
Ssc.16629	NM_001001532	CCR7	Chemokine (C-C motif) receptor 7
Ssc.15861	NM_214126	CD40LG	CD40 ligand
Ssc.42649	NM_001044531	CD70	CD70 molecule
N/A	NM_001244523	CSF1	Colony stimulating factor 1 (macrophage)
Ssc.382	NM_214118	CSF2	Colony stimulating factor 2 (granulocyte-macrophage)
Ssc.16151	NM_213842	CSF3	Colony stimulating factor 3 (granulocyte)
Ssc.35257	NM_001008691	CXCL10	Chemokine (C-X-C motif) ligand 10
Ssc.72492	NM_001128491	CXCL11	Chemokine (C-X-C motif) ligand 11
Ssc.26221	NM_001009580	CXCL12	Chemokine (C-X-C motif) ligand 12

Ssc.80308	XM_003356973	CXCL2	Chemokine (C-X-C motif) ligand 2
Ssc.26146	NM_001114289	CXCL9	Chemokine (C-X-C motif) ligand 9
Ssc.38900	XM_003133651	CXCR2	Chemokine (C-X-C motif) receptor 2
Ssc.7176	NM_213773	CXCR4	Chemokine (C-X-C motif) receptor 4
Ssc.15870	NM_213806	FASLG	Fas ligand (TNF superfamily, member 6)
Ssc.63662	XM_003127307	FLT3LG	Fms-related tyrosine kinase 3 ligand
Ssc.4093	NM_213948	IFNG	Interferon-gamma
Ssc.148	NM_214041	IL10	Interleukin 10
Ssc.55412	XM_003129890	IL10RA	Interleukin 10 receptor, alpha
Ssc.15484	NM_213771	IL10RB	Interleukin 10 receptor, beta
Ssc.71	NM_214013	IL12B	Interleukin 12B (natural killer cell stimulatory factor 2, cytotoxic lymphocyte maturation factor 2, p40)
Ssc.15877	NM_213803	IL13	Interleukin 13
Ssc.8833	NM_214390	IL15	Interleukin 15
Ssc.18652	NM_213751	IL16	Interleukin 16

UniGene	GenBank	Symbol	Description
Ssc.42770	NM_001005729	IL17A	Interleukin 17A
Ssc.51662	XM_001924366	IL17F	Interleukin 17F
Ssc.20	NM_213997	IL18	Interleukin 18 (interferon-gamma-inducing factor)
Ssc.15792	NM_214098	IL-18RA	Interleukin-18 receptor alpha chain
Ssc.113	NM_214029	IL1A	Interleukin 1, alpha
Ssc.28829	NM_214055	IL1B	Interleukin 1, beta
Ssc.16250	NM_214262	IL1RN	Interleukin 1 receptor antagonist
Ssc.26323	NM_214415	IL21	Interleukin 21
Ssc.56047	NM_001130236	IL23A	Interleukin 23, alpha subunit p19
Ssc.36782	NM_001007520	IL27	Interleukin 27
Ssc.15739	NM_214083	IL2RG	Interleukin 2 receptor, gamma
Ssc.15837	NM_214123	IL4	Interleukin 4
Ssc.17244	NM_214340	IL4R	Interleukin 4 receptor
Ssc.528	NM_214205	IL-5	Interleukin 5
Ssc.69951	XM_003358500	IL5RA	Interleukin 5 receptor, alpha
Ssc.62	NM_214399	IL6	Interleukin 6 (interferon, beta 2)
Ssc.16374	NM_214403	IL6R	Interleukin 6 receptor
Ssc.25033	NM_001097432	IL6ST	Interleukin 6 signal transducer (gp130, oncostatin M receptor)
Ssc.15904	NM_214135	IL7	Interleukin 7
Ssc.47709	NM_001146128	IL7R	Interleukin 7 receptor
Ssc.658	NM_213867	IL8	Interleukin 8
Ssc.51687	NM_001166043	IL9	Interleukin 9
Ssc.52878	NM_214402	LIF	Leukemia inhibitory factor (cholinergic differentiation factor)
N/A	XM_001929161	OSM	Oncostatin-M-like
Ssc.21207	XM_013995322	IL17B	Interleukin-17B-like
N/A	XM_005660112	IL33	Interleukin-33-like
Ssc.102621	NM_001260482	TNSF14	Tumor necrosis factor ligand superfamily member 14-like
Ssc.50114	XM_003124679	IL9R	Interleukin-9 receptor-like
N/A	XM_013995322	LOC1006216 82	Interleukin-24-like
Ssc 88958	XR_304407	IL2RB	Hypothetical protein LOC100621776
Ssc.27595	NM_214453	LTA	Lymphotoxin alpha (TNF superfamily, member 1)
Ssc.15277	NM_001185138	LTB	Lymphotoxin beta (TNF superfamily, member 3)
Ssc.551	NM_001077213	MIF	Macrophage migration inhibitory factor (glycosylation-inhibiting factor)
Ssc.22083	NM_001031793	NAMPT	Nicotinamide phosphoribosyltransferase
Ssc.23321	NM_214023	SPP1	Secreted phosphoprotein 1
Ssc.10287	XM_003130499	TGFB2	Transforming growth factor, beta 2
Ssc.100	NM_214022	TNF	Tumor necrosis factor
Ssc.90180	XM_001927216	TNFRSF11B	Tumor necrosis factor receptor superfamily, member 11b
Ssc.94376	NM_001024696	TNFSF10	Tumor necrosis factor (ligand) superfamily, member 10
Ssc.47270	NM_001097498	TNFSF13B	Tumor necrosis factor (ligand) superfamily, member 13b
Ssc.23487	NM_001025217	TNFRS4	Tumor necrosis factor (ligand) superfamily, member 4
Ssc.57541	NM_214084	VEGFA	Vascular endothelial growth factor A
Ssc.10316	XM_003357928	ACTB	Actin, beta
Ssc.73773	NM_213978	B2M	Beta-2-microglobulin
Ssc.16135	NM_001206359	GAPDH	Glyceraldehyde-3-phosphate dehydrogenase
Ssc.4158	NM_001032376	HPRT1	Hypoxanthine phosphoribosyltransferase 1
Ssc.27927	XM_003127305	RPL13A	Ribosomal protein L13a

JPET-AR-2020-000047

Targeted Injection of a Truncated Form of Tissue Inhibitor of Metalloproteinase 3 Alters Post-MI Remodeling

Running Title: TIMP-3 domains and post-MI remodeling

David C. Lobb, PhD[+], Heather Doviak, BS[+], Gregory L. Brower, PhD[+], Eva Romito, PhD[+], Jason W. O'Neill, PhD[§], Stephen Smith, PhD[§], James A. Shuman, MD[+], Parker D. Freels, MD[+], Kia N. Zellars, BS[+], Lisa A. Freeburg, BS[+], Aarif Y. Khakoo, MD[§], TaeWeon Lee, PhD[§], Francis G. Spinale, MD, PhD[+]

[+]Cardiovascular Translational Research Center, University of South Carolina School of Medicine and the WJB Dorn Veteran Affairs Medical Center, Columbia, SC; [§] Amgen, Metabolic Disorders, South San Francisco, CA

Supplemental Figure 1. Histochemistry of Post-MI Remote Regions

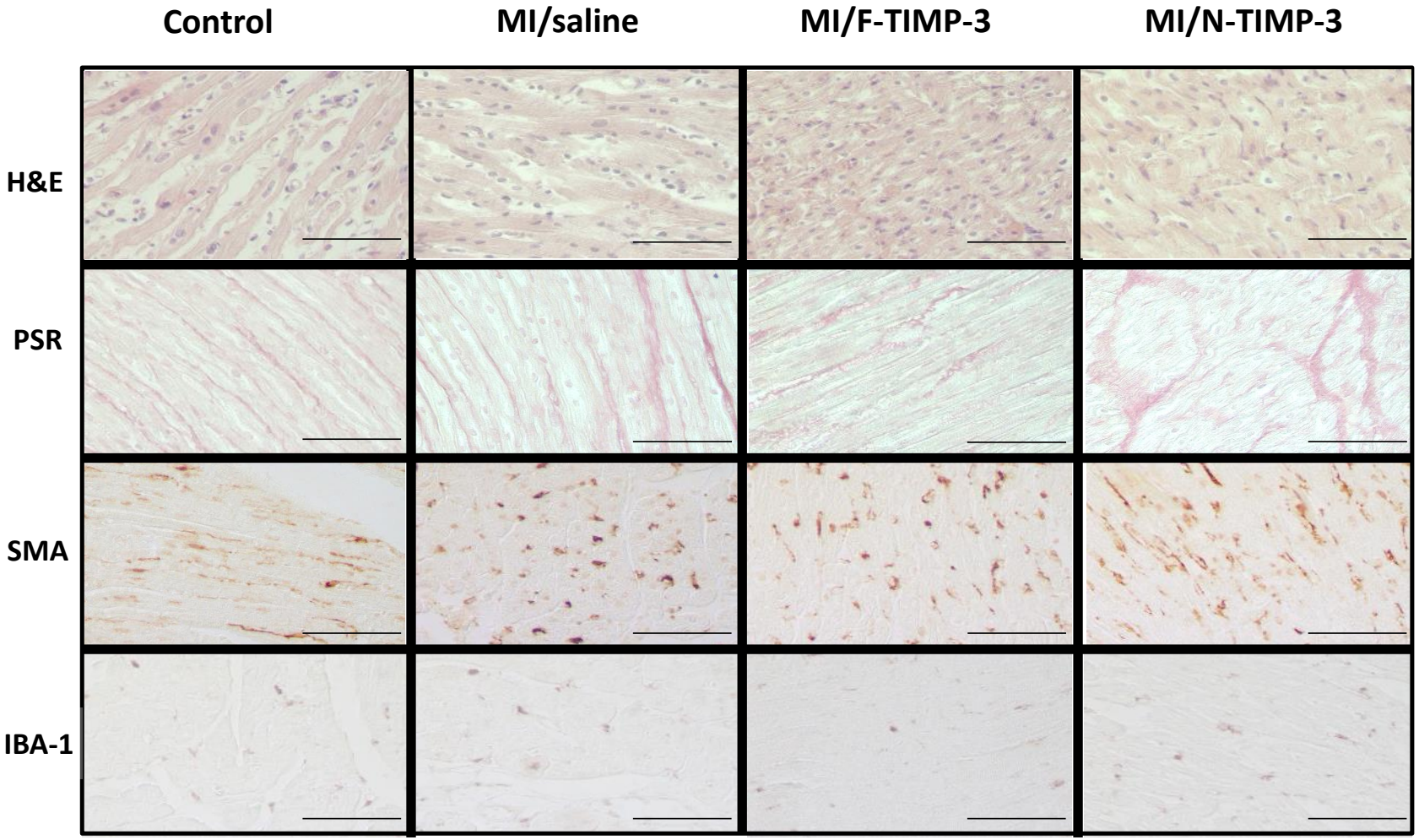

(TOP) H&E sections revealed normal myocardial architecture within remote region. PSR stained sections revealed clear bands of fibrillar collagen within the remote region in all post-MI groups. SMA and macrophage staining (IBA antibody) revealed a minimal positive signal in the referent normal and remote samples. (Original magnification 40X, bars=100 um).

JPET-AR-2020-000047

Targeted Injection of a Truncated Form of Tissue Inhibitor of Metalloproteinase 3 Alters Post-MI Remodeling

Running Title: TIMP-3 domains and post-MI remodeling

David C. Lobb, PhD[+], Heather Doviak, BS[+], Gregory L. Brower, PhD[+], Eva Romito, PhD[+], Jason W. O'Neill, PhD[§], Stephen Smith, PhD[§], James A. Shuman, MD[+], Parker D. Freels, MD[+], Kia N. Zellars, BS[+], Lisa A. Freeburg, BS[+], Aarif Y. Khakoo, MD[§], TaeWeon Lee, PhD[§], Francis G. Spinale, MD, PhD[+]

[+]Cardiovascular Translational Research Center, University of South Carolina School of Medicine and the WJB Dorn Veteran Affairs Medical Center, Columbia, SC; [§] Amgen, Metabolic Disorders, South San Francisco, CA

Supplemental Methods

Recombinant TIMP-3 Protein Synthesis and Validation

Human F-TIMP-3 was expressed in Chinese hamster ovary cell lines using a vector with a Cytomegalovirus promoter, whereby conditioned media was concentrated by tangential flow filtration (TFF; Millipore,10kD MWCO) and then filtered (Fractogel EMD SO3; Merck KGaA, Darmstadt, Germany). The F-TIMP-3 was eluted (0.1 M NaCl gradient) and purified by size-exclusion chromatography (Ni-NTA resin, Qiagen, Valencia, CA). The F-TIMP-3 containing fractions were concentrated by TFF and buffer exchanged (10 mM Na Acetate pH5.2, 9% Sucrose). The 13-KDa N-TIMP-3 was purified in a similar manner in E.coli whereby the sequence was from the N-terminus to Glycine 120 residue. A global MMP fluorescent peptide assay was next performed whereby the MMP substrate (60 μM; Omni MMP Substrate, BML-P126, Enzo) and a recombinant active MMP enzyme (10 nM; BIOMOL, SE-237/SE-244) were incubated in the presence and absence of increasing concentrations of F-TIMP-3 or N-TIMP-3. Fluorescence of the cleaved substrate was measured, (280/360 nm; FLUOstar, BMG Laboratories) whereby inhibition in MMP activity occurred with increasing concentrations of either F-TIMP-3 or

N-TIMP-3 with an approximate 50% inhibitory concentration (IC_{50}) of 2-6 ug/mL (0.4-5 nM), indicative that both proteins inhibited MMP activity.

Dose Ranging Studies

The 6-point injection pattern allowed for the 2 TIMP formulations and the 3 dilutions to be used in each pig, whereby the pattern of injection was alternated with each pig. At 3 (n=5) or 5 (n=5) days following injection, the animals were deeply anesthetized with isoflurane (5%), the targeted LV injection region removed and placed in iced saline, and the 6 injection transmural injection sites separated. The LV samples were homogenized and then subjected to protein separation (25 µg LV extract protein/lane) by electrophoresis followed by immunoblotting using an affinity purified monoclonal antibody against human TIMP-3 (Abcam ab 61316; 1:3000-F-TIMP-3/1:1000 N-TIMP-3 dilution). The recombinant F- and N-TIMP-3 were used as positive controls, and as this antibody has no cross-reactivity, did not recognize native porcine TIMP-3, and thus non-injected porcine LV myocardium served as a negative control. In order to buttress the immunoblotting approach, a human TIMP-3 ELISA (Accusignal, Rockland Inc, Cat # KOA0315) was also used on these LV extracts (25 ug/sample/well). Using the internal standards and linear curve fitting the optical densities (450 nm, SpectraMax), the actual concentrations of the injected TIMP-3 constructs were computed. All of these measurements were performed on all of the injected LV samples and performed in triplicate.

All of the immunoassay reagents utilized antisera raised against human F/N-TIMP-3 and did not react against native porcine TIMP-3. A positive immunoreactive signal based upon positive recombinant controls was observed, whereas there was an absence of an immunoreactive signal using non-injected LV pig extracts (Figure 1C). These studies identified that with F-TIMP-3 injections, a strong signal was observed at 5 mg injections and that LV saturation occurred with N-TIMP-3 injections at 2-5 mg concentrations. Quantitation was carried out on these LV injection sites using a human specific ELISA and demonstrated a stepped increase in F-TIMP-3 from 2-10 mg injections. Using these results, and to ensure dosing equivalency with respect to mass/volume, a 5 mg/injection dose was selected for subsequent in-vivo studies. Using the 6-point injection pattern yielded a total myocardial delivery of 30 mg of either F- or N-

TIMP-3. While absolute myocardial concentration computations require several assumptions, the total injected myocardial region was 4 mL (2X2X1 cm, specific gravity of 1 cm^3/mL), resulting in an initial delivery of 750 ug/mL, thus reflective of a 100X concentration from the computed EC_{50} for the TIMP formulations.

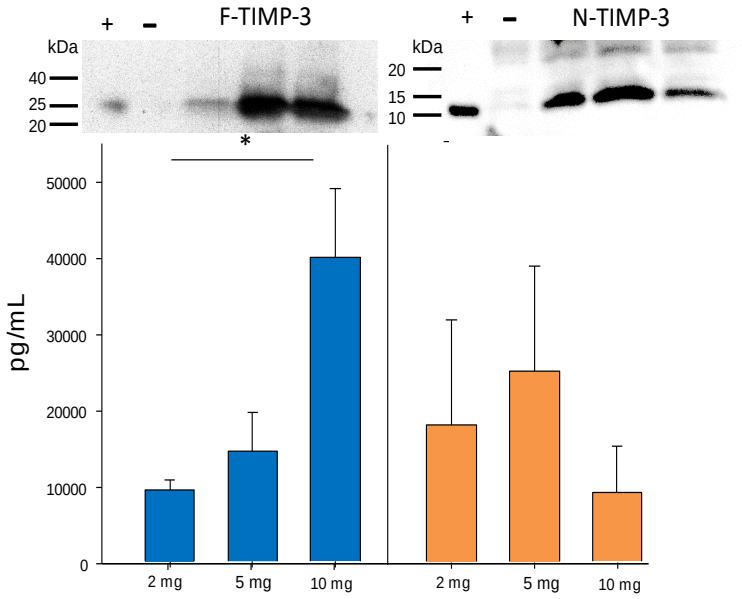

Shown above are representative immunoblots of LV myocardial samples collected at 3 days following a targeted injection array containing either F-TIMP-3 or N-TIMP-3 (2-10 mg/injection site). Equivalent LV extract protein concentrations (10 µg /lane) were used, and F-TIMP-3 or N-TIMP-3 (10 µg) were also used as positive control (+) whereby non-injected LV extracts were used as negative (-) controls. The antisera used in these studies were anti-human and did not cross react with native porcine TIMP-3 and thus were used to initially examine the localized augmentation of TIMP-3. These studies identified that with F-TIMP-3 injections, a strong signal was observed at 5 mg injections and that LV saturation occurred with N-TIMP-3 injections at 2-5 mg concentrations. Quantitation was carried out on these LV injection sites using a human specific ELISA and demonstrated a stepped increase in F-TIMP-3 from 2-10 mg injections (*$p<0.05$ vs 2 mg). Using these results, and to ensure dosing equivalency with respect to mass/volume, a 5 mg/injection dose was selected for subsequent in-vivo studies.

Fluorescent Labelling of TIMP-3 Constructs

F-TIMP-3 or N-TIMP-3 were fluorescently labelled with IRDye800 by diluting to 2.5 mg/mL of the respective TIMP-3 in 50mM Sodium Borate, pH8.0, 50mM NaCl, 2mM

EDTA, 5% Trehalose, and adding approximately 4X molar excess of Dylight800 (20mM Stock in DMSO, ~2% final, DyLight 800 NHS ester, Thermo Scientific). The reaction was incubated for 1.5hr at 37^{o}C, and 200mM L-Arginine was then added to prevent aggregation and subjected to column separation (Sephadex G25 column with PBS, pH 7.4). The final labelled TIMP-3 formulation was prepared by dialysis (overnight in PBS), and confirmation of labelling was established by analytical size exclusion chromatography (@ 280nm vs 777nm). Following injection and the specific time point, LV sections were subjected to epi-illumination imaging (Xenogen IVIS, PerkinElmer, Inc, MA). The settings for the imaging system were predicated upon the IRDye800 spectra (745/800 ex/em) and the signal collected over a 0.5 sec exposure window. The digitized images (Living Image Software, PerkinElmer Inc., MA) were then subjected to planimetry (Image J Software, Research Services Branch, MD) in order to determine the total LV circumferential area for that region, and the final results expressed as the area occupied by fluorescent TIMP-3. A representative set of LV images from each region with injection of each TIMP-3 formulation immediately following injection and at 3 and 5 days post-injection is shown in Figure 1D. Using an exponential fit model, the computed F-TIMP-3 retention half-life was approximately 8 days, and for N-TIMP-3, it was approximately 6 days.